CREEP BEHAVIOR OF HIGH-PERFORMANCE CONCRETE REINFORCED WITH POLYPROPYLENE FIBERS

By

ANDREW SHEHATA

A thesis submitted to the

School of Graduate Studies

Rutgers, The State University of New Jersey

In partial fulfillment of the requirements

For the degree of

Master of Science

Graduate Program in Civil & Environmental Engineering

Written under the direction of

Hani Nassif

And approved by

____

____

____

New Brunswick, New Jersey

May 2019

ABSTRACT OF THE THESIS

Creep Model Predictions for High-Performance Concrete with Polypropylene Fibers

By ANDREW SHEHATA

Thesis Director:

Dr. Hani H. Nassif

High performance concrete (HPC) is being used on daily basis by the construction industry, due to its suburb properties. HPC attains high strength and durability that made it out preform other concrete mixes. With the extensive use of HPC in all type of infrastructures, challenges tended to arise, and shrinkage issues became obvious, and accelerated curing was needed by the construction industry. Shrinkage in HPC resulted into cracking, which made the steel reinforcement in all the structures vulnerable to corrosion. Fiber reinforcement in concrete became one of the practices to minimize shrinkage cracks, and avoid corrosion concerns. Moreover, accelerator admixtures started gaining popularity because it allowed faster construction, which resulted in shorter traffic closures, as well as lowering construction costs.

Effects on creep and shrinkage behaviors with the use of fibers and accelerator liquid admixtures in HPC remains in question. Although fiber reinforced HPC and high early strength (HES) concrete is being frequently used, there is not enough research preformed to understand their creep and shrinkage phenomena.

The objective of this research study is to investigate the effects of polypropylene fibers and accelerated admixtures to creep and shrinkage deformations in HPC. Several theoretical models will also be modeled, analyzed and evaluated with comparison to the experimental results. Finally, adjustments to the models will be suggested to improve creep predictions.

ACKNOWLEDGEMENTS

The following thesis was completed under the guidance of Professor Hani H. Nassif of the department of Civil and Environmental Engineering. I would like to thank Dr. Nassif for providing me the opportunity to work with him as an undergraduate and graduate research assistant and the constant encouragement and support during the progression of writing this thesis.

I would also like to thank Dr. Adi Abu-Obeidah, and Dr. Hao Wang for being members of my committee.

I would also like to thank the undergraduate research assistants for the significant amount of help provided throughout the experimental stage of the research including mixing, testing and maintenance work. I would especially like to show my gratitude for Dr. Adi Abu-Obeidah who, since my very first day of research, has served as a great mentor and supervisor with his experience and knowledge.

Finally, I thank my family and friends for their care and love throughout my time here at Rutgers University.

TABLE OF CONTENTS

ABSTRACT OF THE THESIS ii

ACKNOWLEDGEMENTS iv

LIST OF FIGURES ix

LIST OF TABLES xi

CHAPTER I 1

1. INTRODUCTION 1

1.1 PROBLEM STATEMENT 1

1.2 REASEARCH OBJECTIVES AND BACKGROUD 3

1.3 THESIS ORGANIZATION 4

CHAPTER II 6

2. LITERATURE REVIEW 6

2.1 Introduction 6

2.2 High-Performance Concrete (HPC) 6

2.3 Shrinkage 9

2.4 Creep 11

2.5 Fibers 13

2.6 Chemical Admixture 16

2.7 Factors Directly Influencing Creep and Shrinkage 17

2.7.1 Concrete Materials 17

2.7.1.1 Aggregate 17

2.7.1.2 Cement 18

2.7.1.3 Fly Ash 18

2.7.1.4 Slag 19

2.7.1.5 Accelerator 20

2.7.1.6 Water Content 20

2.7.1.7 Water to Cement Ratio 21

2.7.2 Environmental Factors 21

2.7.2.1 Relative Humidity 21

2.7.2.2 Temperatures 22

2.7.3 Loading Factors 22

2.7.3.1 Age of Concrete 22

2.7.3.2 Shape of Structure 23

2.8 Prediction Models Assumptions 24

2.8.1 Shrinkage and Creep are additive 24

2.8.2 Linear Aging Model 25

2.8.3 Separation of Creep into Basic and Drying Creep 25

2.9 Prediction Models 26

2.9.1 ACI 209R 26

2.9.2 Bazant Baweja B3 Model 27

2.9.3 CEB MC90-00 Model 28

2.9.4 GL2000 Model 29

2.9.5 Models Notes 29

CHAPTER III 33

3.1 Introduction 33

Fabrication procedure 34

3.3 Material Properties 35

3.4 Mix Design and Procedure 36

3.4.1 Mix Preparation 39

3.4.2 Mix Procedure 40

3.4.3 Fresh Property Testing 41

3.4.4 Sampling and Casting Procedure 43

3.4.5 Curing and Storage 44

3.5 Mechanical Property Tests 45

3.5.1 Compressive Strength Testing 45

3.5.2 Tensile Strength Testing 47

3.5.3 Elastic Modulus Testing 49

3.5.4 Free Shrinkage Testing 49

3.5.5 Rapid Chloride Permeability 51

3.5.6 Surface Resistivity 52

3.6.1 Creep and Shrinkage Set Up 53

3.6.1 Creep and Shrinkage Testing Procedure 55

3.6.1 Creep and Shrinkage Data Collection 58

CHAPTER IV 61

4.1 Introduction 61

4.2 Fresh Concrete Tests Results 61

4.3 Compressive Strength 62

4.3 Tensile Strength 64

4.4 Elastic Modulus 66

4.6 Free Shrinkage 68

4.5 Surface Resistivity 69

4.5 Rapid Chloride Test 70

4.6 Shrinkage Strains and Specific Creep. 71

4.6.1 Comparison of HPC Mixes 71

4.6.2 Comparison of HPC-HES Fly Ash Mixes 72

4.6.3 Comparison of HPC-HES Slag Mixes 73

4.6.4 Comparison of HPC and HPC-HES Concrete Mixes 74

4.6.5 Comparison of HPC-HES-FA and HPC-HES-SL Concrete Mixes 76

CHAPTER V 77

5.0 Models VS Experimental Specific Creep 77

5.1 Models VS Experimental Creep: HPC, HPC-HES-FA and HPC-HES-SL Plane Mixes 78

5.2 Models VS Experimental Creep: HPC, HPC-HES-FA and HPC-HES-SL Fiber Reinforced Mixes: 80

5.1 Conclusion 82

CHAPTER VI 84

6.0 Bibliography 84

LIST OF FIGURES

Figure 2-1: Creep and Shrinkage Behavior (Bazant 1994)	11
Figure 2-2: 2-in Macro Polypropylene Fibers	16
Figure 3-1: 6 x 12 Free Shrinkage and Creep Cylinder Mold	35
Figure 3-2: Concrete Mixer	39
Figure 3-3: Slump Test	42
Figure 3-4: Air Content Pressure Device	42
Figure 3-5: Casted Specimens	43
Figure 3-6: Environmental Chamber	44
Figure 3-7: Compressive Strength Test	46
Figure 3-8: Forney Compression Machine	46
Figure 3-9: Tensile Strength Test	47
Figure 3-10: Tensile Failure Mechanism for Plain Mixes	48
Figure 3-11: Tensile Failure Mechanism for Fiber Reinforced Concrete	48
Figure 3-12: Compressometer Cage	49
Figure 3-13: Free Shrinkage Test	50
Figure 3-14: RCPT Test	51
Figure 3-15: Surface Resistivity Test	52
Figure 3-16: Rig Assembly (Nassif 2003)	54
Figure 3-17: Creep Rig (Nassif 2003)	54
Figure 3-18: VWSG Attached to the 6 x 12 Cylinders	57
Figure 3-19: Creep Cylinders Tower	57
Figure 3-20: Hydraulic Jack Placement for Loading	58
Figure 3-21: Campbell Scientific Loggernet System	60
Figure 4-1: Compressive Test Results for 4 x 8 cylinders	63
Figure 4-2: Tensile Test Results for 4 x 8 cylinder	65
Figure 4-3: Elastic Modulus Test Results	67
Figure 4-4: Free Shrinkage Test Results	68
Figure 4-6: HPC Specific Creep	71
Figure 4-5: HPC Free Shrinkage	71

Figure 4-7: HPC-HES-FA Free Shrinkage 72
Figure 4-8: HPC-HES-FA Specific Creep 72
Figure 4-9: HPC-HES-SL Free Shrinkage` 74
Figure 4-10: HPC-HES-SL Specific Creep 74
Figure 4-12: HPC-FA VS HPC-HES-FA SC 75
Figure 4-11: HPC-FA VS HPC-HES-FA FS 75
Figure 4-12: HPC-HES-FA VS HPC-HES-SL FS 76
Figure 4-13: HPC-HES-FA VS HPC-HES-SL SC 76
Figure 5-1: HPC-FA-CR Models VS Experimental 78
Figure 5-2: HPC-HES-FA-CR Models VS Experimental 78
Figure 5-3: HPC-HES-SL-CR Models VS Experimental 78
Figure 5-4: HPC-FA-FR Models VS Experimental 80
Figure 5-5: HPC-HES-FA-FR Models VS Experimental 80
Figure 5-6: HPC-HES-SL-FR Models VS Experimental 80

LIST OF TABLES

Table 2-1: Creep Models Variables	31
Table 2-2: Statistical Analysis Results (Al-Manaseer et al. 2005)	32
Table 3-1: Material and Supplies	36
Table 3-2: Concrete Mix Designs	37
Table 4-1: Fresh Concrete Test Results	61
Table 4-2: Compressive Test Results for 4 x 8 cylinder	62
Table 4-3: Compressive Test Results for 6 x 12 cylinders	64
Table 4-4: Tensile Test Results for 4 x 8 cylinder	65
Table 4-5: Elastic Modulus Test Results	66
Table 4-6: Surface Resistivity Test Results	69
Table 4-6: Surface Resistivity Test Results	70

CHAPTER I

1. INTRODUCTION

1.1 PROBLEM STATEMENT

High-performance concrete (HPC) is defined by ACI as concrete that has been designed to be more durable and, if necessary, stronger than conventional concrete. Even though, HPC and conventional concrete are composed of the same essential materials, but the variation in material proportions and mixing process significantly effects the mechanical properties. HPC mixes are engineered to optimally and efficiently provide enhanced durability, reduced permeability, and higher strength at an economic cost compared to conventional concrete. Even though HPC offers great mechanical properties, it is susceptible to cracking, due to low water to cement ratio (w/c). Cracking is a major problem to all concrete structures because it leads to corrosion of the reinforcements, in which lead to dramatically shortens the life span of the bridges.

Used as a substitute to plane HPC, fiber reinforced concrete has been gaining popularity in recent years. Fiber reinforcement has been gaining popularity in the recent years due to its enhancement to concrete's properties, in terms of shrinkage resistance, tensile strength and toughness. Fibers are offered in different sizes and materials, such as polypropylene, steel and glass. Each fiber type has its own advantages and disadvantages, for that reason, fiber type is determined based on the concrete's mix application.

Different fibers have different properties, therefore, the type of fiber used in a concrete mix depends on the concrete's application.

Due to the economic losses caused by traffic closures for construction, there was a high demand for high early strength concrete. Moreover, during staged construction of bridge deck repairs, traffic on adjacent lanes develop tension strains in newly poured concrete. Induced strains in early stages of construction mitigated cracks on new bridge decks, due to NSC slow strength development. Therefore, researchers developed High Early Strength (HES) concrete which is one of the HPC categories. Since HPC-HES is designed mainly for highway applications, water to cement ratio (W/C) is minimized to avoid frost complications. However, HPC-HES shared the same disadvantages of HPC concrete, which is their cracking tendency (Castine 2017).

All types of concrete infrastructures are subjected to sustained dead loads, which causes the creep phenomena. Creep is defined by ACI 209 as a periodic increase in strain due to sustained stresses. Shrinkage and swelling strains caused by the environment, as well as elastic strains induced as a result of loading are not included in creep. a permanent deformation that takes place when concrete experience constant stress for a period of time. Creep deformation derive an increase in structures' deflection, cracking and loss of pre-stressing force which all results in shortening the life span of infrastructures. Fully understanding the behavior of creep and shrinkage is essential for design purposes, but the phenomena are complex as stated by ACI 209 (Aïtcin 1998). Moreover, the popularity of fiber reinforced concrete, and HPC-HES concrete, further complicate the challenge of understanding the behavior of the phenomena. To overcome the challenge of creep and shrinkage phenomena additional research needs to be conducted. Due to the importance of creep deformation for design purposes, more research need to be done to improve the understanding of creep strain with the use of deferent concrete mixes, with deferent types of reinforcement.

1.2 REASEARCH OBJECTIVES AND BACKGROUD

The goal of this research is to investigate the creep and shrinkage behavior of HPC concrete with the use of polypropylene fibers, and the addition of accelerating admixtures, with fly ash (FA) and slag (SL) as partial replacements. Moreover, this experimental study will test the creep Through the experimentation process, fiber material, size and quantity will stay constant as well as aggregates type, and amount. Afterwards, collected creep results will be compared to models for plane HPC mixes. Data collected will be compared to ACI 209R-92, Bazant Baweja B3 ,CEB MC90-00 and GL2000 models, and specific suggestions will be made to improve the current models. Detailed analysis will be done to understand the performance of the ACI 209R-92, Bazant Baweja B3 ,CEB MC90-00 and GL2000 creep models in comparison to the experimental creep of plain and fiber reinforced HPC and HPC-HES concretes. Moreover, proper adjustments to the models will be suggested based on investigations preformed, to account for the use of accelerating admixtures and polypropylene fibers in concrete. All materials used for mixing were gathered in a cost effective manner locally within New Jersey, while ensuring high quality standard concrete that meets all ACI specifications, and practical for construction purposes. All mixes tested shared the same aggregate and cementitious types and sizes.

1.3 THESIS ORGANIZATION

This thesis has six chapters as followed:

Chapter I:

A brief introduction and background of the purpose and goals of this research study is provided.

Chapter II:

Literature review of high performance concrete, fiber reinforcement in concrete, creep and shrinkage phenomena, variables effecting creep and shrinkage will be discussed. Moreover, a concise explanation will be provided on the following ACI creep models: ACI209R-92, Bazant Baweja-B3 Model, CEB MC 90-99, and GL2000 Model.

Chapter III:

Review of all the concrete mixes analyzed and experimental testing performed for this research study will be provided. Creep and shrinkage test setup, and testing and data collection steps will be discussed.

Chapter IV:

A discussion of the analyzed results obtained from immediate, mechanical properties, creep and shrinkage tests will be provided. Comparison of creep and shrinkage behavior of each concrete mix. Evaluation of the fiber reinforcements, addition of accelerators, and the use of fly ash and slag as partial replacements for cement in terms of creep and shrinkage.

Chapter V:

Comparison between creep and shrinkage experimental data and ACI current prediction models

Chapter VI:

Conclusion of this research study, suggestions and recommendations to improve the creep models. Possible future work to continue creep deformation investigation.

CHAPTER II

2. LITERATURE REVIEW

2.1 Introduction

A literature review will be provided in this chapter on HPC and HPC-HES concrete mixes discussing their unique properties, applications and shortcomings. and on creep and shrinkage phenomena. Moreover, a detailed explanation on creep and shrinkage phenomena and the variables effecting both behaviors will be reviewed. Furthermore, a concise exploration of ACI 209R-92, Bazant Baweja B3,CEB MC90-00 , GL2000 models will be discussed. Finally, the variables that the creep and shrinkage models take into consideration will be clarified and the variables that the models lake to consider will be addressed

2.2 High-Performance Concrete (HPC)

Up to 1960's the concrete industry and structural engineers were satisfied with the concrete material in the industry, with strength of 2,175 to 2,900 psi (Aitcin 1998). Only in in the mid 1960's few researchers believed that concrete can be effectively optimized to achieve higher strength. At that time fly ash (FA) and water reducers (WR) were newly introduced to the concrete's industry in North America. FA is a fine grained material that is used as a partial substitute for cement to achieve higher strength concrete. WR is a chemical admixture added to the concrete during the mixing process to increase concrete's workability while keeping the water to cement ratio (w/c) low (Hover 1999). At that time WR were significantly varied in their composition and purity, as a result, the concrete's performance was noticeably varied. After serious research efforts were invested in optimizing concrete, the industry realized the importance of FA and WR. The utilization of FA and the introduction of WR allowed the possibility of further developing the strength of concrete. This time in history was the beginning of the development of High Strength Concrete (HSC). Periodically the concrete industry improved their understanding of concrete as a complex composite material, and were able to optimize the use of FA and WR admixtures in concrete.. By 1970's HSC reached a compressive strength of 8700 psi, and the industry could not exceed that strength anymore. WR that were available at that time were not capable of further lowering the water/cement ratio in the concrete mixtures. Moreover, even though the concrete's strength was dramatically increased, but the designers were not impressed by the performance of HSC due to its low durability (Aitcin 1998).

By 1970's HSC reached a compressive strength of 8700 psi, which the industry struggled to exceed. This plateau was a result of the WR's inability to further lower the water/cement ratio in the concrete mixtures. The low durability of the HSC overpowered the concrete's increased strength, which left the designers unimpressed by the performance of the concrete (Aitcin 1998).

The development of HPC started with the establishment of plasticizers, and their usage in concrete mixtures. Plasticizers are liquid admixtures that allowed to further reduce the water/cement ratio, therefore, increasing concrete's strength, while improving the durability of concrete. Later the performance of HPC concrete was further improved by the introduction of silica fume (SF) to the concrete industry (Brewer 2018). The performance of HPC concrete was even further improved when silica fume (SF) was introduced to the concrete industry (Brewer 2018). With the proper proportions of cement, FA, and SF, and with the correct amount of plasticizers, HPC concrete reach a compression strength of 19,000 psi (Aitcin 1998). The satisfaction of the construction industry with the capabilities of HPC was due to it high performance and not necessarily it's high strength. Due to the use of fine cementitious materials used in HPC concrete, it has very low porosity and permeability. Therefore, the use of cementitious materials in HPC makes the mixture highly resistible to weathering actions, chemical attacks, and deterioration (Khadiranaikar et al.). Furthermore, the use of plasticizers in HPC concrete, improves HPC's workability resulting in ease in casting and lowering construction costs.

Due to the superb performance and properties of HPC, it has been increasingly used in construction. The high strength that HPC offers, allows designers to use smaller size members, and less steel reinforcement. As a result, HPC became the optimal concrete mix for concrete infrastructures, because it is economically efficient and also provides useable space under bridges, and in buildings. Moreover, HPC concrete gains early age strength, which allows constructions acceleration, and further reduce construction costs. However, cracking was still a major issue with HPC concrete, because the penetration of water and oxygen progresses the corrosion to the concrete reinforcement.

Recently, accelerated bridge constructions became more popular and used more frequently. In accelerated bridge construction projects, accelerator admixtures are used in the concrete, to reach high early strength (HES). The disadvantages of HPC-HES concrete, is its low slump and low durability in terms of cracking (Castine 2017). The use of plasticizers can offset the low slump, but cracking still remains a problem.

As a result, fiber reinforcement in HPC mixes gained popularity, and thousands of papers were published clarify the effects of fibers in HPC.

2.3 Shrinkage

Any concrete type experience two types of deformations. The two types of strains that concrete experience are additive. First type of strain that concrete encounter is Shrinkage, and the second type is Creep. The Shrinkage is defined as the deformation of concrete due to the loss of moisture (Farrington et al. 1964). Shrinkage causes a change in volume and shape of structures without placing any stresses on the concrete (Farrington et al. 1996). Early age shrinkage takes place in three phases, which are autogenous, drying and thermal. Long term shrinkage is carbonation, thermal, chemical and autogenous.

Autogenous happens due to the demand of water in the concrete during the hydration process. Autogenous shrinkage take place without any loss of moisture content to the atmosphere, and it causes a decrease in the volume of concrete (Lluka et al. 2015).

Drying Shrinkage occurs as a result of the loss of water content to the atmosphere. During the process of curing the concrete, drying shrinkage can dramatically increase if the specimens are not kept in a room with 100% humidity (Lluka et al. 2015). It is also important to note that the change in volume of the concrete samples does not equal to the change of the moisture content in the mixture (Farrington et al. 1996).

Concrete expands and shrinks with fluctuation of temperatures. Thermal shrinkage takes place in concrete as any other material when concrete is casted or is being cured in cool climate. On the other hand, concrete expansion can occur as a result of increase in concrete's temperature due to heat of hydration, or due to the acceleration of concrete hardening by the addition of accelerating admixtures (Acker 2001).

Finally, carbonation shrinkage happens due to the reaction of the heat of hydration products with carbon dioxide in the atmosphere. In this process carbon dioxide from the atmosphere reacts with calcium hydroxide in the concrete to produce calcium carbonate which results in shrinkage of the concrete structure. Carbonation shrinkage is excessive when the relative humidity is between 40% and 70% (Acker 2001).

Shrinkage must be closely monitored and evaluated to properly understand creep's behavior. The concrete deformation due to shrinkage have to be separated from the deformation caused by creep, in order to better understand the behavior of HPC mixes.

2.4 Creep

Creep in concrete was discovered in 1907 by HATT, and since then creep has been a major field of research for all types of concrete mixtures and infrastructures (Shah et al. 1971). Creep phenomena is an inelastic deformation that results from sustained loads. Basic creep of concrete can also be defined as the difference between loaded and load-free concrete samples and structures as shown in figure 2-1. Load free concrete specimens undergoes considerable permanent deformations due to drying shrinkage (Bazant 2001). Loaded concrete specimens experience drying shrinkage which is the total strain of concrete due to applied stresses and free shrinkage. Basic creep strain is the deformation the concrete undergoes due to the applied loads only, and that can be calculated by the subtraction of drying creep by the drying shrinkage (Bazant et al. 1994).

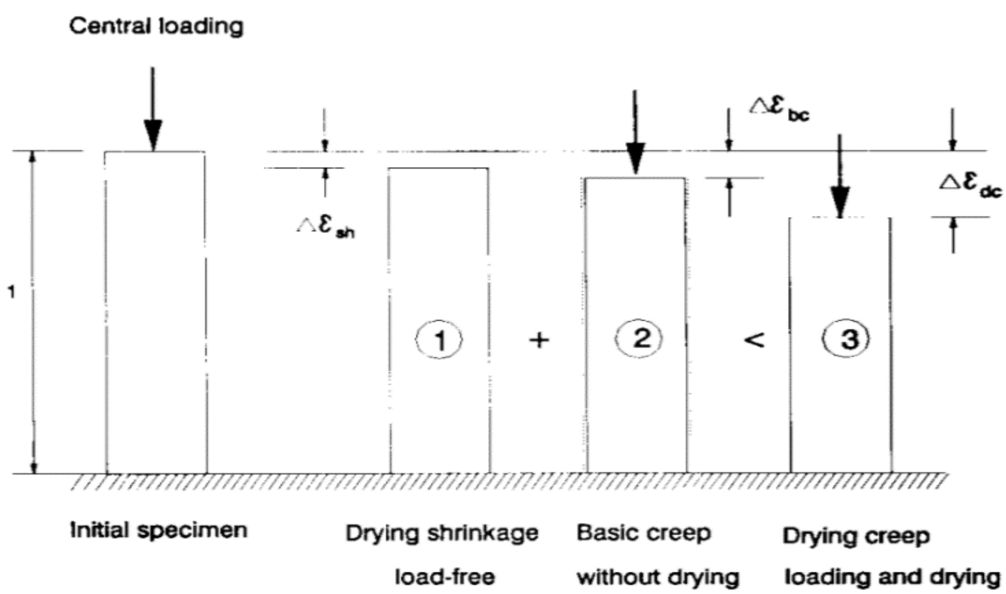

Figure 2-1: Creep and Shrinkage Behavior (Bazant 1994)

Concrete creep strains usually takes place in the direction of the load, and it results in a change of the shape of the structure. Moreover, creep deflections causes an increase in bending moments, which can lower the buckling strength and bearing capacity of concrete columns (Bazant 1968). Creep strains are effected by various factors such as level of stress, strength of concrete, temperature, humidity, size of member, time of loading, time under loading, and multi-axial loading (Bazant 2001).

High stress levels cause an increase of shrinkage and creep deformation, therefore, understanding creep behavior heavy construction is essential. Creep strain in bridges is a concern that engineers always have to keep in mind during the design process, because it effects the stability of bridges especially if it is a pre-stressed bridge (Sagara et al. 2015). Bridge deformations due to creep result in loss of pre-stress force which lowers the design strength of bridges. Creep deformation in tall buildings can cause major structural actions in horizontal members, due to the shortening of vertical members as a result of creep. Therefore, creep strain can cause significant changes in members' design stresses that can result in failures (Chowdhary et al. 2013). Furthermore, the effects of creep and shrinkage can result in excessive amount of deformation as well as the spread of wide cracks in a structure (Rajeev et al. 2007). In reinforced concrete columns, creep strain results in transfer of stress from concrete to the steel reinforcement. In any concrete infrastructure if steel reinforcement reaches its maximum stress capacity, the element will fail in a brittle behavior. Usually in any concrete structural element engineers purposely design concrete to fail before steel reinforcement to take advantage of steel's ductility and allow more time for evacuation. Creep deformation can disturb the failure mechanism designed for an infrastructure. Even thought, knowing the creep deformation is necessary for the design of concrete bridges, the estimation of it is still approximate and uncertain. Moreover, with the use of high strength and pre-stressed concrete in today's industry more accurate methods need to be used to obtain the proper creep and shrinkage stains in concrete structures (. With that said, creep can be of some benefit when stress relief is necessary. In the cases of changes in temperature, foundation and shrinkage movements, creep can relieve stresses in concrete and prevent cracking (Dilger).

2.5 Fibers

Fibers have been introduced to the concrete industry 1960s, and has been gaining an exceeding attention since then (Zollo 1998). When fibers were first introduced to the concrete industry, high expectations were set to improve the performance of Portland Cement. Researchers had hopes that the use of fibers a dramatic improvement in Portland cement's brittle matrix will occur. Research was limited at that time due to the limited fiber production. Initial testing showed that fibers can be a beneficial addition to concrete mixtures, which encouraged companies to invest more in fibers production. By mid 1980s fibers were available in many materials and with different sizes (Zollo 1998). Fibers are now offered in various materials and each type has its own advantages and disadvantages. Fibers material and size is usually chosen based on nature of the project. Mostly used fibers are steel, polypropylene, and glass. Moreover, fiber behavior also depends other factors such as concentration, dispersion and orientation. Fiber reinforcement was proven to improve concrete's tensile and flexural strength, as a result, enhance concrete's resistance to crack propagation (Shah et al. 1971). Furthermore, fiber reinforcement reduces permeability in concrete, therefore offering a longer life span for concrete structures. This study will investigate the creep performance of HPC reinforced with polypropylene

Synthetic fibers have been increasingly used in construction. Synthetic fibers are offered in two categories: micro and macro fibers, and they are categorized by their length. Micro fibers are added to concrete to reduce early age cracking. Macro fibers enhances the structural performance of concrete, in terms of flexural strength and toughness, and they are typically longer or equal to 1.5 inches (Barborak 2011). Moreover, Macro polypropylene fibers have been attracting attention due to their low cost and weight. Research showed that polypropylene fibers improve concrete's resistance to acid and corrosion. Polypropylene fibers reinforcement enhances concrete's toughness and resistance to shrinkage cracks (Sohaib et al. 2018). Even though it is arguable that fiber steel reinforcement can majorly enhance concrete's performance better than polypropylene, but the inherent corrosive tendency of steel fibers, had made both materials competitive (Gregory 2018). On the other hand, the plasticity of polypropylene fibers makes it easy to spread though out the concrete mixture, and rule out clustering problems. The use of polypropylene fibers will also rule out any corrosion concerns.

Many research studies had shown that fibers reinforcement dramatically effects creep strain in normal strength concrete (NSC). It was proven that then higher the elastic modulus the fibers possess the lower the creep deformation, and vice versa. Experimental studies showed that 2% of volumetric blending of fiber steel reinforcement can lower creep by 25.1% in 365 days due to its high elastic modulus. On the other hand, 2% of volumetric blending of polypropylene can increase creep deformation by 19.9% (Zhao 2015). At the same time, an experimental work done by J, Houde, A. Prezeau, and R.

Roux to test the effects of steel and polypropylene fibers in normal strength concrete for creep deformation. The study included concrete mixes with 1.0% and 0.3% per volume of steel and polypropylene fibers respectively. All specimens were cured for 7 days in moist conditions. Results indicated an increase of creep strain up to 40% for steel fibers, and 20% increase for polypropylene fibers (Houde et al. 1987). In conclusion, results do not look consistent and further research needs to be done to clarify the behavior of creep in fiber reinforced concrete mixtures.

The addition of polypropylene fibers creates extra sliding in the concrete which softens the structure and causes extra deformation under stresses (Jarosaw 2017). With the development of HPC concrete in the industry, HPC was examined for creep strain and compared to NSC ACI models. Results showed that HPC concrete undergoes 60% less creep deformation over a period of 120 days compared to NSC ACI models. Due to the rigidity of HPC concrete creep deformation is limited, but that can restrict HPC structures stress relieve which increase the probability of cracking (Dilger). Research showing creep effects of fiber reinforced HPC is still lacking. It is essential to understand effects of creep on HPC concrete, because the high strength that HPC concrete attains makes it more brittle, therefore, the addition of fibers is important. Effort was made in this paper to analysis creep behavior of Polypropylene fiber reinforced HPC. Shown in figure 2-2 are 2 inches Polypropylene macro fibers used for this research. The goal of this research effort is to take advantage of HPC concrete, and polypropylene fibers unique properties in one concrete mixture, in hope of experiencing lower creep deformation than of polypropylene fiber reinforced NSC.

Figure 2-2: 2-in Macro Polypropylene Fibers

2.6 Chemical Admixture

Superplasticizers are used in concrete to improve the workability of concrete and especially if the concrete being casted has low w/c ratio like all high strength concretes. A side advantage of the use of High Range Water Reducers (HRWR) is the increase of concrete's strength, and the reduction of concrete's free shrinkage (Whiting 1987). However, even though it seems like HRWR improves concrete's durability, it was reported by Tynes (Whiting 1987) that concrete contacting HRWR failed in freezing and thaw testing. A research study performed by CTL supporter Tynes experimental work and showed an increase in coarseness of the air-void size distribution in the concrete (Whiting 1987)

Air entraining admixtures' main purpose is to eliminate air voids in concrete mixes with low w/c ratio. Air voids in concrete stabilizes air voids and improves concrete's freeze and thaw durability (Du et al. 2005). Therefore, the use of air entraining admixtures over comes the only disadvantage the concrete industry faces with the use of superplasticizer. Research studies have also shown that air entraining admixtures do not affect the shrinkage or creep of concrete (Davis and Troxel, 1954).

2.7 Factors Directly Influencing Creep and Shrinkage

2.7.1 Concrete Materials

2.7.1.1 Aggregate

Material properties and quantity of aggregate, cementitious materials and admixtures used in concrete mixes, have direct effects on creep behavior. High aggregate volumes in concrete mixtures tend to lower creep in infrastructures (Branson et al. 1971), that is a result of the natural behavior of aggregate which does not undergo any creep deformation under stress. It also been found that the type and porosity of the aggregate used effect the creep of concrete, because aggregates with higher porosity usually have a lower modulus of elasticity. If the aggregate has low modulus of elasticity that means that it deforms more under stress, which increases creep. Red Sandstone, Green Sandstone, Marble, River Gravel, Granite and Quartz have high absorption, therefore, they have low modulus, and high strains under stress (Neville et al. 1964). Moreover, the use of well graded aggregate helps decreases creep deformation, because it assists in minimizing the voids in the concrete.

2.7.1.2 Cement

Cement types only have considerable influence on creep of concrete at early stages. Different types of cements react at different rates, therefore, effecting the early strength of concrete. Creep deformation is lowered as the strength of concrete decreases. Type III, and I gains high early strength respectively, thus, Type III experience the lease creep at early stages compared to Types I. However, if specimens were loaded at 28 days using Types I and III, minimal creep effects will be observed, because both mixes would have already gained most of their strength (Neville et al. 1964). Other types of cement are used in construction applications where low heat of hydration or high sulfate resistance is required, and they usually take much longer time to react.

2.7.1.3 Fly Ash

The use of Fly Ash (FA) in concrete has been dramatically increasing due to its technical and economic advantages as a cementitious material. FA has various benefits in concrete's mechanical properties if used in the correct proportions (Sennour 1989). The use of FA as cement substitute can improve the workability, lower early heat of hydration, improve freezing and corrosion resistance, and refine permeability of concrete (Zhang et al. 2012). Moreover, using FA in concrete was a main factor in the creation of high strength concrete (Zhao et al. 2015). FA concrete undergoes less free shrinkage as well, due to the low w/c ratio which decreases the amount of evaporated moisture (Ghosh 1981). It was proven that due the strengthening of concrete with the use of FA, creep strains decrease as a result of the decrease of the stress/strength ratio (Zhao et al. 2015). Furthermore, Yuan and Cook (1983) tested various concrete mixes with different FA contents and they concluded that 20% FA replacement has the optimum creep result.

2.7.1.4 Slag

Slag is another type of cementitious material that can partially replace cement to improve the performance of concert. Slag cement is manufactured by grounding granulated blast furnace slag (GGBFS) to a fine particle that can benefit concrete's properties, and it separated into three grades. The three grades of slag are Grade 80, Grade 100, and Grade 120 and are determined based on the slag activity test, which is found using compression strength of the slag-reference cement (GCP Applied Technologies 2016). The addition of slag in concrete enhances the compressive and flexural strength, durability, workability, and lowers the permeability of concrete when compared to concrete mixes with only Portland cement (Shahab 2017). Strength gaining is relatively slow in concrete mixtures with slag cementitious, therefore, there is no advantage of slag in terms of strength within the first 28 days. Moreover, slag effectiveness in concrete is highly dependable on the curing process. Concrete containing slag is best cured using water (Shahab 2017). Concrete containing slag experience almost the same amount of shrinkage as cement base concrete, but less shrinkage than cement base concrete on the long run. Tazawa, Yonekura, and Tanaka's experimental work also showed that the specific creep of slag concrete was almost the same as specific creep of non-slag concrete, when specimens were casted for 28 days (Tazawa et al. 1989).

2.7.1.5 Accelerator

There are various types of accelerating chemical admixtures, and different types develop early strength of concrete in a different manner, therefore, it is challenging to define the term “accelerator”. One of the most acceptable concepts of an accelerator is that it promotes a higher rate of formation of hydration products. Most of the other types of agents produce insoluble reaction products which as a result of an immediate reaction that take place between the accelerating agent and the calcium hydroxide in the liquid phase of the cement paste. Both processes help quickly increase the solid to liquid ratio, therefore, assist in hardening of the concrete, and gaining early strength (Rosskopf 1975). Publications on the effects of accelerators to concrete’s shrinkage and creep deformations has been limited. Brooks and Neville (Brooks et al. 1992) did tests for type C and E accelerating admixtures containing calcium chloride. Results of the research testing concrete mixes containing accelerating admixtures showed an increase of basic of 122% to 133%, 131% to 203% of drying creep, and 133% of shrinkage. Type C non chloride admixture indicated an increase of 110% to 125% of basic creep, 92-135% of drying creep and 110% of shrinkage for plain concrete (Brooks et al. 1992).

2.7.1.6 Water Content

Moreover, water content has major effects on creep behavior. The popular theory of seepage that is accepted by most scientist, in which volume of concrete changes due to the squeezing of water pores out of the specimens, when external load is applied (Theiner et al. 2017). Therefore, exposed structures experience more seepage, because a dramatic loss in water content is lost to the atmosphere under stresses, allowing excessive creep deformation (Theiner et al. 2017). Various research studies have indicated that water content extraction from concrete specimens always decreases creep deformation (Tamtsia et al. 2000). Unsealed concrete samples with admixtures experience 4.21 times more creep strains than sealed specimens (Al-Manaseer et al. 1986). Moreover, Brown and Hope (Brown et al. 1976) concluded that concrete elements with all evaporable water being extracted experience no creep strains.

2.7.1.7 Water to Cement Ratio

Water to Cement ratio (W/C) has a significant effect on creep of concrete. It was proven though Wagner and Hummel experimental work that an increase in the W/C results in higher creep deformations. Their research effort included concrete mixes with w/c varying from 0.35 to 0.9, and the result showed that the specimens with 0.35 w/c ratio had the lowest creep strains. High w/c ratio lowers the strength of concrete dramatically, therefore, it has negative effects on creep deformations. Moreover, high w/c ratio increase the content of active water which is defined by (El Khoury 2010) as the water redistribution under high stresses, causing creep deformation.

2.7.2 Environmental Factors

2.7.2.1 Relative Humidity

As a result of the importance of water content for creep of concrete, relative humidity is essential. Relative air humidity controls the rate of diffusion of moisture from the concrete. If concrete structures are exposed to low relative humidity, then the loss of water pores from the concrete structure will be rapid. Fast loss of water content from the concrete to the environment causes an increase in drying shrinkage and seepage which increases creep deformations (Khoury 2010). Therefore, relative humidity has major effects on creep deformation. It was proved that relative humidity has inverse effects on creep strains. Concrete structures subjected to high humidity has higher resistance to creep deformation, as it lowers the escape of moisture content from the concrete (Chowdhary et al. 2013).

2.7.2.2 Temperatures

Environmental temperature has significant effects on creep strains. High temperatures influence the physical and chemical reactions in the concrete's cement past, which effect the dehydration of the concrete's matrix. The dehydration of casted concrete effect the plastic strain of the specimens due to the development of macro and micro cracks. Crack initiated due to dehydration increase creep deformations (Schneider 1988). Moreover, the water mobility mechanism, also suggest an increase in creep strains with increased temperatures at early age (Hauggaard et al. 1999). The water mobility mechanism demonstrates a decrease in viscosity for increased microprestress, which results in higher strain rates (Hauggaard et al. 1999).

2.7.3 Loading Factors

2.7.3.1 Age of Concrete

Age of concrete has a direct proportionality to creep of concrete. When concrete is cured for longer periods it gains higher compression strength which results in lower creep deformations. Therefore, age of loading is significant to creep strains (Nemati 2006). Moreover, age of loading is directly related to the evaporable water content, which effects creep strains. Older specimens contain less evaporable water; therefore, they exhibit less creep (Niyogi et al. 1973).

Older concrete specimens have higher strength therefore, have lower creep deformations (He 2013). Polivka (1964) experimental study included creep testing of samples at various ages, and the results showed 18% more creep for concrete specimens cured for 1 day compared to 3 days after 28 days of loading. Concrete gain more strength at older ages due to the effect of the hydration process. The effects of concrete strength on creep strains is neglible for concrete with 28 days of curing or higher (Sennour 1989).

2.7.3.2 Shape of Structure

Hatten and Mattock (1966), discovered that the variation in size and shape of concrete structures at all ages affect creep strains. Larger concrete structures experience less creep deformation and at a lower rate. Creep for large exposed structures can correspond to basic creep of sealed members. Hatten ad Mattock (1996) tested different size samples for shrinkage and creep, and their results showed that a cylinder with 24 in diameter, and length of 58in, experienced final shrinkage strain of 500με. On the other hand, another sample with 4in diameter and length of 18 in undergo 938με of shrinkage strain. The noticeable difference in shrinkage accompanied with the varied sizes directly affect the drying creep deformation of concrete structures.

2.8 Prediction Models Assumptions

Prediction models are necessary due to the long term effect of creep and shrinkage on concrete infrastructures. Research efforts developed prediction models to expect the behavior of various concrete mixtures with different mixing and loading procedures. Creep and shrinkage are influenced by many factors such as concrete strength, concrete's age, aggregate type and volume content, type of curing conditions, humidity and temperature conditions, w/c ratio, type of concrete, structure's dimensions, type of loading and loading period (Rajeev et al. 2007). Therefore, all mentioned variables have to be included in creep and shrinkage model predictions to improve long term behaviors of concrete structures. Up to early 1980's computer technologies were limed for computations, therefore the first prediction models were based on Effective modulus method, Age-adjusted effective modulus method, Double power law for creep and double power logarithmic law. Starting the 1980's researchers developed more advanced models using computer computational methods such as ACI-209R-82 model, CEB-FIB model code 1990, B3 model, Mulled model, and GL2000 model, that were backed up by various research and experimental studies (Rajeev et al. 2007). All prediction models discussed in the chapter follow the same standard testing conditions, and the same simplified assumptions for creep and shrinkage deformations.

2.8.1 Shrinkage and Creep are additive

Concrete mixtures are casted in to two set of specimens, and are cured in the same environmental conditions. Strains are monitored and collected for one set of samples without being loaded, just to analyze shrinkage. External loads are applied on the second set of specimens and strains are collected as well. Creep strains due to applied loads are then calculated by subtracting the strains of the loads free samples from the strain of the loaded samples. Therefore, creep and shrinkage strains are considered independent of each other and additive (ACI 209.2R 2008).

2.8.2 Linear Aging Model

Research showed that as long as the applied stresses to the concrete are less than 40% of the compressive strength, stresses and creep are approximately proportional. In other words, superposition principle can be applied to calculate total strain responses, for increasing and decreasing stresses. However, with the use of superposition principle for creep strain calculations, all reversal strains such as relaxation have to be excluded (ACI 209.2R 2008).

2.8.3 Separation of Creep into Basic and Drying Creep

Creep deformation is divided into basic creep and drying creep. Basic creep is a material property which is independent of the structure shape of size. Basic creep is monitored and measured by applying stress to sealed specimens to avoid ingress or egress of any moisture content from the samples to the environment. Drying creep is measured by loading unsealed specimens and subtracting elastic, shrinkage and basic creep deformations from the total strain collected from the unsealed samples. The unsealed specimens with applied external loads have to be in a temperature controlled environment for avoid and thermal expansion or shrinkage. If samples are not in temperature controlled environment, then thermal strains have to be collected and subtracted from the strain of the unsealed specimens to properly calculate drying creep (ACI 209.2R 2008)

2.9 Prediction Models

2.9.1 ACI 209R

The model ACI 209R was first developed by Branson and Christiason , and it was recommended by ACI Committee 209 in 1971. The model was originally designed for precast-prestressing industry. ACI 209R-82 made minor changes in 1982, then the model was later updated in 1992 and was never revised after (ACI 209.2R 2008). The model is applicable for normal and light weight concrete. Moreover, the model can be used for concrete mixes cured using moist and steam methods. ACI 209R provisions are appropriate for concrete mixes with type I and II cement only (Rajeev et al. 2007). ACI 209R-92 model is known for its simplicity, however, the data predictions offered by the model is limited. The model is can easily be modified using ultimate shrinkage or creep to match short term experimental data. On the other hand, the method of accommodating member size is limited in its accuracy specially when it is used in its basic forms. Moreover, ACI 209R-92 cannot model shrinkage or creep phenomena because it is based on empirical data. The model only requires the age of concrete after curing ends, age of concrete at loading, curing method, relative humidity, volume-surface ratio, and cement type. ACI 209R-92 assumes an elastic modulus value which can cause issues when calculating creep coefficient. Furthermore, the model underestimates high shrinkage values, and overestimated low shrinkage values (ACI 209.2R 2008).

2.9.2 Bazant Baweja B3 Model

The development of the Bazant Baweja model started in the 1970s. The model was mathematically created based on more than 10 physical phenomena that have direct effects on creep and shrinkage. The B3 model is special because it deals complex and simple structures. Moreover, Bazant Baweja model utilizes the use of compliance function to reduce errors to improve the accuracy of the elastic modulus of the concrete (ACI 209.2R 2008). The model was recommended by RILEM TC-107-GSC. Bazant Baweja B3 model is restricted to concrete mixes with mean compression strength between 1740 to 11600 psi at 28 days, mean relative humidity between 40-100% and mean temperature between 41-86 Fahrenheit. he model also gives separate values for basic and drying creep strains (21). Factors included in Bazant Baweja B3 model:

1) concrete's age after moist curing ends
2) age of concrete at loading
3) aggregate content in concrete
4) Cement in concrete
5) Cement type
6) Mean compressive strength at 28 days
7) Curing method
8) Relative humidity expressed as a decimal
9) Shape of specimen
10) Volume- Surface ratio
11) Water content in concrete

Bazant Baweja B3 model also have default values and equations that can be used to if the user is missing some of the information needed.

2.9.3 CEB MC90-00 Model

CEB MC90-99 model first started in 1990 by Muller and Hilsdorf to predict creep and shrinkage in concrete. The model was first updated in 1999 to separate autogenous and drying shrinkage, and to add normal and high strength concretes, and was named CEB MC90-99. Some engineers prefer using this model over ACI 209R-92 (ACI 209.2R 2008). Any changes in the relative humidity can cause a dramatic change in the correction term for relative humidity in the creep equations used in this model. Parameters needed for this model are as following:

1) concrete's age after moist curing ends
2) Age of concrete at loading
3) Mean compressive strength at 28 days
4) Relative humidity expressed as a decimal
5) Volume surface ratio
6) Cement type

It was proven that CEB MC90-99 model underestimates shrinkage for North American concrete, and dramatically under estimates concretes made with basalt aggregate brought from New Zealand, Hawaii, and Australia (ACI 209.2R 2008).

2.9.4 GL2000 Model

GL2000 model was invented in 2001 by Gardner and Lockman and was later modified in 2004. The model is an updated version of Atlanta 97 model to follow ACI 209 model guidelines. All of the factors needed for the model are available for designers, except for the concrete mean compression strength at 28 days (ACI 209.2R 2008). The model can be used for concretes with compression strength less than 10150 psi, and with w/c ratio between .4 and .6 (Rajeev et al. 2007). Parameters needed to use this model are listed below:

1) concrete's age after moist curing ends
2) Age of concrete at loading
3) Mean compressive strength at 28 days
4) Relative humidity expressed as a decimal
5) Volume surface ratio
6) Cement type

2.9.5 Models Notes

Results from all models discussed were compared to RILEM data bank. Bazant-Baweja B3 and GL2000 calculated the closest shrinkage results to that of RILEM databank. GL2000, CEB MC90-99 and Bazant-Baweja B3 provided the best compliance prediction models. On the other hand, ACI 209R-92 model underestimated most of the compliance data of the RILEM databank. The addition of parameters in the models improved the prediction methods in all the models except for ACI209R-92. The results from CEB, GL2000, and Bazant-Baweja B3 were dramatically improved when the concrete strength was updated by measuring the strength development elastic modulus of the concrete. When GL2000 and Bazant-Baweja B3 methods were analyzed, calculations showed that the shrinkage prediction between both models were within 20% and 30% for compliance. All discussed models proved that the super position principle can be used to calculate concrete relaxation as long drying calculations are kept constant before loading (ACI 209.2R 2008). All the models discussed consider different variables as shown in table 2-1, but none of the models account for fiber reinforced concrete, or for the use of liquid admixtures such as accelerators in the shrinkage and creep calculations.

	ACI 209R-92 Model	Bazant-Baweja-B3 Model	CEB MC90-99 Model	GL2000 Model
Concrete Data				
Specified 28 days strength	✓	✓	✓	✓
Ambient Conditions				
Relative humidity	✓	✓	✓	✓
Temperature			✓	
Specimen:				
Volume-to surface ratio	✓	✓	✓	✓
Shape		✓		
Initial Curing				
Curing time		✓		✓
Curing condition		✓		
Concrete at loading				
Age at loading	✓	✓	✓	✓
Applied stress range			✓	
Estimated Concrete Properties				
Mean 28 days strength	✓	✓	✓	✓
Strength constant			✓	
Mean 28 days elastic modulus		✓	✓	✓
Estimated Concrete Mixture				
Cement type	✓	✓	✓	✓
Maximum aggregate size				
Cement content		✓		
Water content		✓		
Water-cement ratio		✓		
Aggregate-cement ratio		✓		
Fine aggregate percentage	✓			
Air content	✓			
Slump	✓			
Unit weight of concrete	✓			

Table 2-1: Creep Models Variables

A statistical analysis was performed in 2005 to compare ACI209R-92, B3, CEB MC90-99, and GL2000 models and find the best prediction model for creep (Al-Manaseer et al. 2005). A summary of the results and ratings obtained from the analysis for creep compliance is presented in the table below.

Category	Time range	ACI 209	CEB 90	B3	GL 2000
1. Distribution of residuals					
Positive range	0 to 9000 days	27%	34%	31%	36%
Negative range	0 to 9000 days	73%	66%	69%	64%
Rating of model*		3	1	2	1
2. Residual range outside					
+33 microstrain/ MPa	0 to 9000 days	0.2%	1%	3%	3%
–33 microstrain/ MPa	0 to 9000 days	20%	15%	15%	17%
Rating of model*		3	1	2	3
3. Mean coefficient of variation V_{CEB} %					
	6	48%	37%	36%	35%
Rating of model*		3	2	2	1
4. Mean square error F_{CEB} %					
	6	32%	31%	35%	34%
Rating of model*		2	1	4	3
5. Mean deviation M_{CEB}					
	6	0.86	0.92	0.93	0.92
Rating of model*		3	1	2	1
6. Coefficient of variation ϖ_{B3}					
	—	87%	75%	61%	47%
Rating of model*		4	3	2	1
Number of categories with Rating 1 or 2		1/6	5/6	5/6	4/6

*Rating of model: 1 = performed best; 4 = performed worst.

Table 2-2: Statistical Analysis Results (Al-Manaseer et al. 2005)

As shown in table 2-2, the results of the statistical analysis show that CEB90, B3, and GL200 models give the best predictions, with rating of 5/6,5/6,4/6 respectively creep (Al-Manaseer et al. 2005).

CHAPTER III
EXPERIMENTAL SETUP

3.1 Introduction

Experimental testing was done to analyze and evaluate creep behavior for HPC and HPC-HES concrete mixes with and without fiber reinforcement. Moreover, various tests were performed in accordance to the ASTM standards on different days to obtain the mechanical properties of the mixes. Test preformed were as follow:

- Compressive testing (1, 7, 14, and 28 days)
- Tensile testing (1, 7, 14, and 28 days)
- Modulus of Elasticity (1, 7, 14, and 28 days)
- Free Shrinkage (1, 7, 14-21, 28, 35, and 42)
- Rapid Chloride Permeability (28 and 56 days)
- Surface Resistivity (7, 14, and 28 days)
- Creep (Data collected over 6 months)

Tests necessary to assure that the concrete mixtures met ASTM standards for fresh concrete were also completed such as slump and air content.

Total of six mixes were examined in this research effort, three were plane concrete mixes and the other three were fiber reinforced with 2in polypropylene synthetic fiber. Concrete mixes tested in this research are listed be

1. HPC control mix with FA being a partial substitute for cement (HPC-FA-C).

2. HPC fiber reinforced mix with FA being a partial substitute for cement (HPC-FA-FR).
3. HPC-HES control mix with FA being a partial substitute for cement (HPC-HES-FA-C).
4. HPC-HES fiber reinforced mix with FA being a partial substitute for cement (HPC-HES-FA-FR).
5. HPC-HES control mix with SL being a partial substitute for cement (HPC-HES-SL-C).
6. HPC-HES fiber reinforced mix with SL being a partial substitute for cement (HPC-HES-SL-FR).

Fabrication procedure

In preparation for mixing, appropriate adjustments have to be done to the 6 x 12 creep cylinders. Bolts have to be embedded in five out of the ten 6 x 12 cylinders. Total of six 1-1/4" bolts are embedded at 120 degree angles as show in the figure 3-1 shown below. The top and bottom spacing of the bolts is equal to the height of the vibrating wire strain gages to ensure a smooth fit when placing the gages. One side of the bolt embedded in the cylinder will be cover with concrete and the other side is for the placement of the gages to measure the strains in the concrete. The bolts are tightened on the cylinders by the use of ¼" bolts from the inside and outside of the cylinders, to make sure the bolts do not move during the casting process. The rest of the cylinders are not modified and are casted normally, and will be used for extra elevation when concrete creep specimens are placed on the creep rigs, and the rest of the cylinders will be used for compression tests.

Figure 3-1: 6 x 12 Free Shrinkage and Creep Cylinder Mold

3.3 Material Properties

All the materials used for the research purpose are readily available within New Jersey and are already being used by companies around the state. All the aggregates and the Portland Cement were provided by Clayton Concrete in Edison New Jersey. Slag was provided by LaFarge in Baltimore. Finally, the chemical admixtures and fibers were delivered by BSAF. Table 3-1 summarizes materials and respective suppliers as well as any specific details necessary to acknowledge.

Material	Type(s)	Supplier(s)
Portland Cement	Type 1	Clayton
Silica Fume	Densified	Clayton
Fly Ash	Class F	LaFarge
Slag	Grade 120	LaFarge
Fine Aggregate	Concrete Sand	Clayton
Coarse Aggregate	#5 (1”) and #8 (3/8”) crushed stones	Clayton
Macro Fibers	2” Polypropylene Fibers	Euclid
Water Reducer (WR)	MasterGlenium 7620	BASF
Air Entraining Agent (AEA)	MasterAir AE 100	BASF
Accelerator	MasterSet AC 534	BASF
Workability Retainer	MasterSure Z60	BASF

Table 3-1: Material and Supplies

3.4 Mix Design and Procedure

All samples for tests performed were taken from the same mixture of each concrete type. All samples were taken from the same mix to keep immediate and mechanical properties consistent with the creep specimens. Mix designs for all tested mixtures are shown in the table 3-2.

	HPC-FA-C-L	HPC-FA-FR-EUC-L	HES-FA-C-L	HES-FA-FR-EUC-L	HES-SL-C-L	HES-SL-FR-EUC-L
SCM	Fly Ash	Fly Ash-Fibers	Fly Ash	Fly Ash-Fibers	Slag	Slag-Fibers
Mixing Date	7/12/2018	7/12/2018	7/19/2018	7/24/2018	11/12/2018	11/14/2018
Creep Loading Dates	Loaded on 8/9/2018	Loaded on 8/9/2018	Loaded on 8/16/2018	Loaded on 8/21/2018	Loaded on 12/10/2018	Loaded on 12/14/2018
Location	Lab	Lab	Lab	Lab	Lab	Lab
Cement, Type II (lb/cy)	520	520	535	535	535	535
Fly Ash, Class C (lb/cy)	130	130	140	140	-	-
Slag, Grade 120 (lb/cy)	-	-	-	-	105	105
Silica Fume (lb/cy)	25	25	25	25	25	25
Total Cement (lb/cy)	675	675	700	700	665	665
#57 (lb/cy)	1,500	1,500	1500	1500	1,500	1500
#8 (lb/cy)	300	300	300	300	300	300
Sand (lb/cy)	1,113	1,113	1,113	1,113	1,113	1,113
MRWR (oz/cwt)	-	-	6.2	5.5	4	5
HRWR (oz/cwt)	5.5	2	-	-	-	-
AEA (oz/cwt)	1	1	1	1	0.1	0.1
Non-Chloride Accelerator (oz/cy)		-	280	280	280	280
Workability Retainer, ViscoFlow 2020 (oz/cy)	-	-	7	7	7	7
Fibers	-	5 lb/cyd (Macro Synthetic Euclid)	-	5 lb/cyd (Macro Synthetic Euclid)	-	5 lb/cyd (Macro Synthetic Euclid)

Table 3-2: Concrete Mix Designs

Three types of concrete mixtures were examined in this research effort, and each type was done once without fibers and once with fibers. The three concrete types are HPC, HPC-HES-FA, and HPC-HES-SL. Each concrete type has its own cementitious, and admixtures mix proportions. HPC concrete mixes' total cementitious were divided into 77% Type I Portland Cement, 19% Fly Ash, and 4% Silica Fume. Water to cement ratio used for HPC concrete was 0.38. Control HPC mix did not contain and fibers and HPC fiber reinforced mix had 5 lb/cy of polypropylene fibers. Only air entraining and water reducer admixtures were used in the HPC mixes. Amount of air entertainer admixture was decided based on the admixture type to reach the proper air content to meet specifications. Similarly, water reducer agent quantities were used as needed to achieve proper slump. For HPC-HES-FA concrete mixes 76% Type I Portland Cement, 20% Fly Ash, and 4% Silica Fume were used of the total cementitious materials used. In terms of aggregate, 52%, 10%, and 38% of #57 aggregate, #8 aggregate, and sand were used respectively. Water to cement ratio for HPC-HES-FA concrete mixes was 0.33. For HPC-HES-SL concrete mixes 80% Type I Portland Cement, 16 % Slag, and 4% Silica Fume were used of the total cementitious materials used. Furthermore, 52%, 10%, and 38% of #57 aggregate, #8 aggregate, and sand were used respectively. Water to cement ratio used was 0.33. For HPC-HES-SL concrete mixes. Moreover, water reducer, air entraining, workability retainer and accelerator admixtures were used in both HES mixes. Proper quantities of liquid admixtures were used based on the admixture's types to achieve the standard specifications for HPC-HES concrete mixes.

3.4.1 Mix Preparation

All aggregates, cementitious, liquid admixtures and water are pre-batched before mixing. Moisture content samples are then collected from the pre-batched buckets, and samples are placed in the oven for at least 3 hours. Pre-batched buckets get sealed to avoid any changes in the moisture content of the batch while moisture content test is being performed. After the moisture content of the fine and course aggregate is found the batch is adjusted to ensure that the desired w/c ratio is achieved. Mixer used in the lab is show in figure 3-2. Maximum capacity of the mixer is 6 cubic feet, therefore, each concrete mix is done in a different day, however, mix proportions are kept the same for each concrete type.

Figure 3-2: Concrete Mixer

3.4.2 Mix Procedure

Mixing then starts by wetting the concrete mixer, and adding all the aggregate but a bucket of sand will be left out for each bucket of cement. The air entraining admixture is then added. The mixer is then closed and turned on for 30 seconds to allow all the aggregate to get mixed properly. Mixer is then moved up to make sure all the course aggregate is at the bottom of the mixer. Half of the batched cement, fly ash and silica fume are added followed with a bucket of sand for each bucket of cement used. Moreover, one half of the total water batched is added to the mix and the mixer is then closed and turned on for 2 minutes. The previous three steps are repeated for the rest of the cementitious materials, sand and water. The water reducer is then added to the mixture to improve the workability of the concrete. After the addition of the water reducer, the mixer is kept closed and turned off for another 2 minutes. To ensure that the water reducer fully reacted with the concrete, the mixer is turned on for 2 minutes. The fibers are slowly and gradually added to the concrete mixture while the mixer is turned on, to make sure the fibers are spread out uniformly in the concrete. Following the addition of the fibers, the mixer is kept sealed and turned on for final 3 minutes. Failures in any of the fresh concrete property tests lead to the addition of chemical admixtures. Concrete is ready to be casted after it is ensured that the mixture passed all ASTM standards.

3.4.3 Fresh Property Testing

Concrete fresh property tests include slump, and air content test. Slump is performed in accordance of ASTM C143 standards. Slump is done by filling the slump cone in one thirds by volume at a time. After each one third of concrete added the layer have to be rodded 25 times using 5/8” tamping rod. Rodding of the concrete layers should penetrate 1 inch of the concrete layer casted previously, and the rod should never hit the hard manor. Following the addition and the rodding of the three concrete layers, all excess concrete at the top of the slump cone is take off and the concrete is levelled. The slump board have to be wiped to make sure no excess concrete is around the slump cone, that can possibly effect the tests’ reading. The slump cone is then slowly raised in a vertical upward motion. Slump reading is then recorded by measuring the difference in height between the concrete sample and the top of the slump cone as shown in figure 3-3.

Air content testing was also done for all concrete mixes in accordance with ASTMC231, using a pressure device presented in figure 3-4. The test is performed by filling a bowel with concrete one third at a time, and concrete is rodded for 25 times after the addition of each layer, similar to the sump test’s procedure. For air content test, after the addition of each concrete layer, the bowel is struck by a mallet 10-15 times all around the bowel. Any excess concrete is the top layer is then removed, and the lid of the pressure device is clamped to the bowel. Water is added to the concrete sample through petcock valves located on the lid, until no more bubbles are seen in the water stream coming out. Valves then are closed and the pressure mark is adjusted by the pump on top of the pressure device lid. The pressure control leveler is then released at the same time the bowel is struck by a mallet. Air content readings are then recorded. After slump and air content tests are preformed and they both pass the standards, the mix is then ready to be casted.

Figure 3-3: Slump Test

Figure 3-4: Air Content Pressure Device

3.4.4 Sampling and Casting Procedure

Specimens casted for testing purposes included 3 prisms, 40 small cylinders, and 10 big cylinders, with dimensions, 3 x 3 x 10, 4 x 8, 6 x 12 inches respectively. Prisms casted are for free shrinkage tests and small cylinders are for mechanical properties tests performed over a period of 28 days. The big cylinders are used to cast creep specimens. During the casting process, all 4 x 8 cylinders are filled half way, rodded, and malleted. Previous step is repeated again and the all excess concrete is removed from the top of the cylinders, leveled with a trowel, and then sealed with proper caps. All 6 x 12 cylinders are caster in a similar fashion but it is casted in 3 layers at a time. The free shrinkage prisms are casted in two separate layers and each layer is rodded and malleted as well.

Plastic wrapping is used to seal the free shrinkage prisms.

Figure 3-5: Casted Specimens

3.4.5 Curing and Storage

After casting is completed, all casted specimens are sealed and placed in the environmental chamber shown in figure 3-6, with a controlled 74 degree Fahrenheit, and 50% humidity environment. After 24 hours, samples are taken out from the chamber to be demolded. After all specimens are demolded, the samples are properly labeled, and cured in 100% moist room for 14 days. Only five 4 x 8 cylinders are placed in a lime water tank. Samples in the lime tank are for RCPT and SR tests.

Figure 3-6: Environmental Chamber

3.5 Mechanical Property Tests

During and after the curing process, various tests were performed to obtain the mechanical properties of the concrete mixes casted. The processes and the method used for all the tests will be discussed in this section.

3.5.1 Compressive Strength Testing

Compressive strength tests were done at 1, 7, 14, and 28 days. For all HPC-HES mixes, extra tests were performed at 6 and 8 hours to obtain the early age strength of the concrete. The testing preformed followed ASTM C39 standards. Compressive strength test is simply done by applying axial load on a 4 x 8 concrete cylinder after it is properly capped. The load applied have to be in an appropriate rate, and is applied till failure of the concrete. The capping of the cylinders is done to ensure that the cylinder is leveled and that the applied load is uniformly distributed on the concrete cylinder. Melted sulfur compound is used in accordance with ASTM C617, and a sample of a capped cylinder is shown in figure 3-7. A one million-pound Forney compression machine show in figure 3-8 was used to perform the compressive tests. At least 2 cylinders are used for each day of testing, if any outliers were noticed, more cylinder get tested.

Figure 3-7: Compressive Strength Test

Figure 3-8: Forney Compression Machine

3.5.2 Tensile Strength Testing

Tensile strength test was performed at the same time compressive strength test was done. A 4 x 8 concrete cylinder is placed horizontally into the Forney compression machine and was tested till it fails in tension in accordance to ASTM C496 as shown in figure 3-8. Loading the specimen was done slowly and at an appropriate rate. Tensile failure was easy to indicate because cracking is usually visible, allowing the sample to split if the concrete mix does not contain fibers 3-9. It was also noticed that specimen with fiber reinforcement failed at a lower rate, and did not completely split at failure as presented in figure 3-10. Similarly, to the compressive test, a minimum of 2 cylinders were tested for tensile strength, and the indication of any outliers resulted in testing more samples.

Figure 3-9: Tensile Strength Test

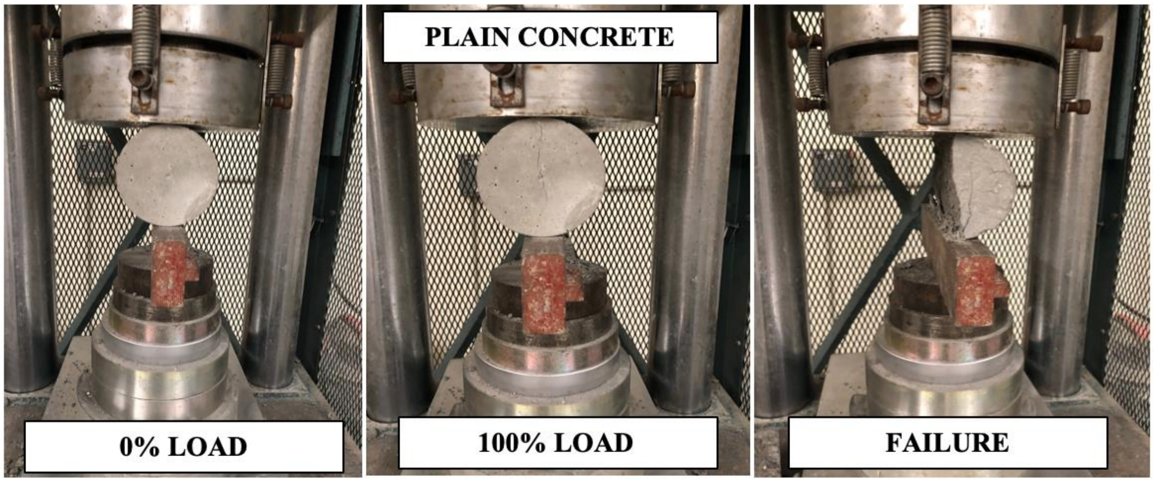

Figure 3-10: Tensile Failure Mechanism for Plain Mixes

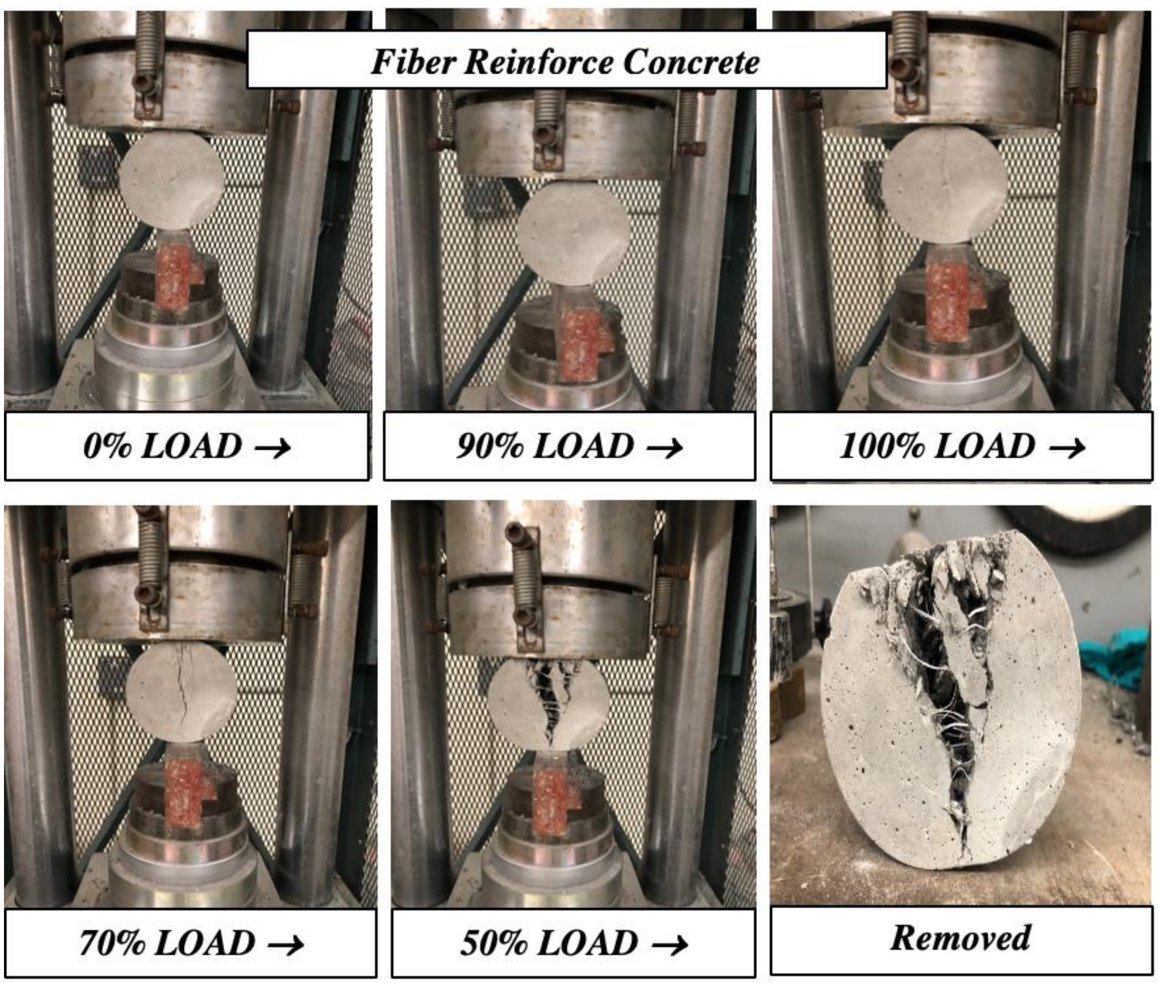

Figure 3-11: Tensile Failure Mechanism for Fiber Reinforced Concrete

3.5.3 Elastic Modulus Testing

Elastic modulus tests were done following the ASTM C469 standards, at the same times as compressive and tension strength tests. Compressive strength test always has to be done before elastic modulus test. The compression strength is need to preform elastic modulus testing. The 4 x 8 concrete cylinders have to be sulfur capped for elastic modulus testing too. A compressometer is then attached to the concrete cylinder by embedding bolts in the concrete through the compressometer cage as shown in figure 3-12. The cylinder is then pre-stressed to 40% of its compression strength. Specimen's vertical height is then measured from opposite sides of the cage using a caliper. The cylinder is the reloaded again to 40% of its compression strength and the reading from the compressometer is recorded while loading. The previous two steps are repeated again. The whole process is re-done for another cylinder. The loads and the compressometer records are used to calculate the elastic modulus of the concrete.

3.5.4 Free Shrinkage Testing

Figure 3-12: Compressometer Cage

Free shrinkage testing was done in accordance with ASTM C157. A total of 3 free shrinkage specimens were casted for each concrete mix. Each sample had a shrinkage gage stud on each side impeded. The prisms were the placed in a free shrinkage apparatus to be tested as shown in figure 3-12. All samples had to be tested directly after being demolded to define their initial dimensions, then placed in a wet tank for curing. All specimens tested for free shrinkage in this research were wet cured for 14 days. The test is then repeated on the mentioned days in section 3.5.1, to monitor the rate of shrinkage over the period of 28 days.

Figure 3-13: Free Shrinkage Test

3.5.5 Rapid Chloride Permeability

Rapid Chloride Permeability (RCPT) test performed to determine the resistivity of the concrete to the penetration of chloride ions. The RCPT test was performed according to the ASTM C1202 standards. The test was done by cutting one of the 4 x 8 cylinders into 2 inches’ discs, and then placing the discs in a vacuum saturation pump apparatus. The apparatus was vacuumed for at least one hour and then the samples were left in the water for approximately 16-20 hours. The disc is then removed from the vacuum apparatus and placed in RCPT cells as shown in figure 3-13. After the discs are tightened in the cells, sodium chloride and sodium hydroxide solutions are added in the appropriate cells. Afterwards, the cells are connected to a computer and the test begin. The tests are performed by passing current through the cells and the concrete discs, and monitoring the permeability of the chloride ions through the concrete. After 6 hours the computer interface monitoring the RCPT test concludes the results of the test. At least 2 samples have to be tested for RCPT for each concrete mix.

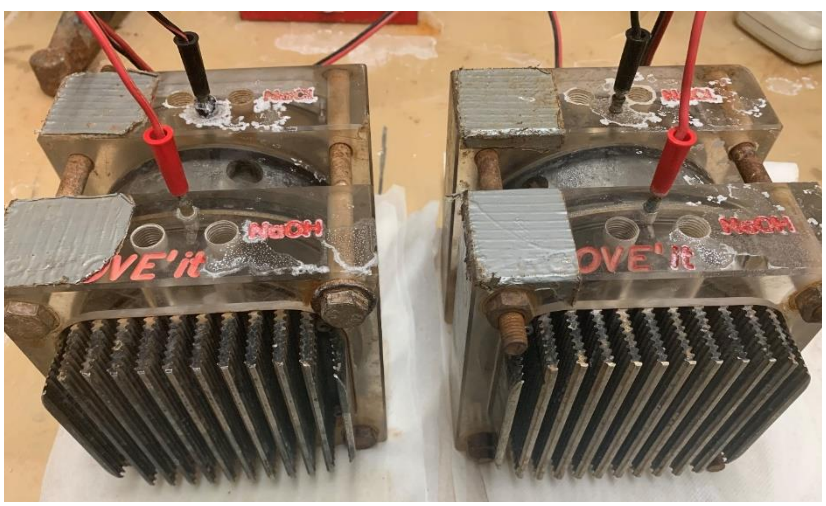

Figure 3-14: RCPT Test

3.5.6 Surface Resistivity

Surface Resistivity (SR) test also has to be done for each concrete mix. The test is done according to the ASTM D257 standards using the Wenner four electrode method. Wenner’s method is performed by pressing four equally spaced electrodes on a concrete cylinder as shown in figure 3-14 in 90 degree increments until 8 reading are recorded. The testing is done for a minimum of 2 cylinders and all values are averaged to find the surface resistivity of the concrete mix. The SR results can be used instead of the RCPT results to find the permeability of the concrete. The SR test is much easier, quicker and is cost effective when compared to the RCPT test.

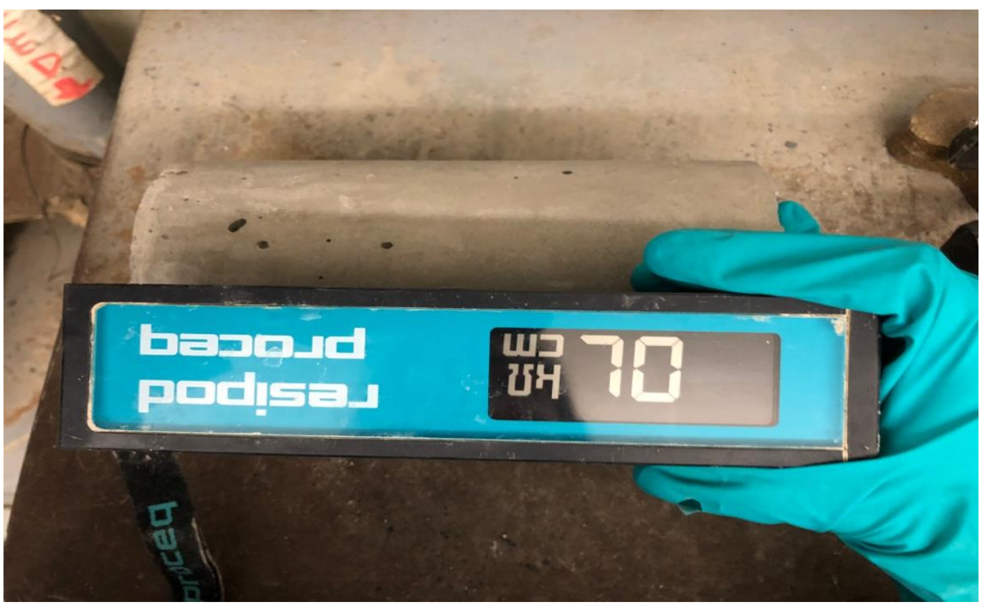

Figure 3-15: Surface Resistivity Test

3.6 Creep and Shrinkage Set Up and Testing Procedure

3.6.1 Creep and Shrinkage Set Up

Eighteen creep rigs are in the environmental chamber in the lab. The chamber is temperature and moisture controlled. The creep rigs are made out of four plates, two with dimensions of 20 x 20 x 2.5 inches, and the other two are 15 x 15 x 2.5 inches. The rigs also consist of four high strength threaded rods, and five double coiled springs. Mentioned parts are assembled as shown in figure 3-16. The 20 x 20 x 2.5 inch plates are placed under and above the springs. The top 20 x 20 x 2.5 plates are allowed to move upward during testing, to apply pressure on the concrete specimens. The other two 15- by 15- by 2.5 inch plates are placed above the concrete cylinders as a cover to restrict any movement during testing. The second 15- by 15- by 2.5-inch plate is used as a jacking platform. The rigs are assembled as presented in figure 3-17 and are designed to fit three 6 x 12 inch, and two 6 x 4 inch cylinders which are cut from a 6 x 12 inch cylinder. A hydraulic jack is prepared to load the rig and the creep cylinders. A Geokon load cell and strain gage meter are prepared to read the applied load during testing.

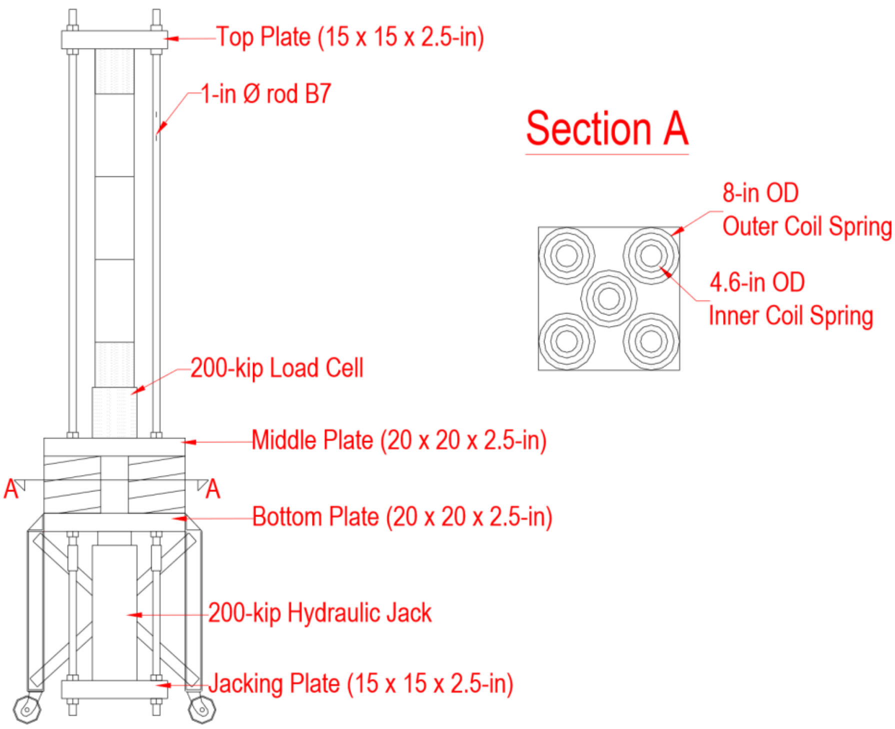

Figure 3-16: Rig Assembly (Nassif 2003)

Figure 3-17: Creep Rig (Nassif 2003)

3.6.1 Creep and Shrinkage Testing Procedure

1) Five 6 x 12 cylinders are removed from the curing room to be properly capped. Three out of the five cylinders will be used to collect creep data and the last two will be used to monitor free shrinkage
2) Afterwards, three vibrating wire strain gages are attached to the bolts embedded in each of the five 6 x 12 concrete cylinders as presented in figure 3-18.
3) Three more 6 x 12 cylinders but without any bolts embedded in them are removed from the curing room. One of those three cylinders is cut into three 4 x 12-inch disc, and two of those discs are sulfur capped and used to elevate the 6 x 4 creep cylinders to fit in the creep rigs.
4) The other two cylinders are tested for compression strength, and the creep cylinders will be loaded up to 35% of the compression strength results.
5) A tower is then built by placing a unit cell, 4 x 8 cylinder, three 6 x 12 cylinder and another 4 x 8 cylinder respectively over each other as shown in figure 3-19.
6) All the cylinders placed on top of each other to build the tower have to be leveled and centered to ensure that all the cylinders are in pure and uniform compression when loaded.
7) Then the top 15 x 15 x 2.5-inch plate is adjusted to be in contact with the top concrete 6 x 4 disc.
8) The hydraulic jack is then placed, centered on the bottom 15 x 15 x 2.5 inches' plate as shown in figure 3-20, and connected to the strain gage meter.

9) After setting up and placing everything in place the nuts on top of the top 20 x 20 x 2.5-inch plate are loosened, as well as the nuts underneath the top 15 x 15 x 2.5-inch plate, to allow space for compression.
10) The last two 6 x 12 cylinders with strain gages connected to them are kept in the environmental chamber were the creep rigs are located, but they will not be loaded, because they are designated for free shrinkage data collection only.
11) Load is the slowly applied to the rig and the creep cylinders, while monitoring the readings of the strain gages to make sure all concrete cylinders are experiencing the same amount of compression.
12) Once the desired load is achieved, the nuts on top of the 20 x 20 x 2.5 in plate and the nuts underneath the 15 x 15 x 2.5 in plates are tightened to the plates. The last step is important because ensures that the load applied on the cylinders is the same and to prevent any eccentricity which can possibly put any of the concrete cylinders' side in tension.
13) The load cell is always monitored to ensure that the rig is re-loaded if the cylinders relaxed and resulted in decreasing the applied stressed. The rig is re-loaded if the desired load decreases more than 2%.

Figure 3-18: VWSG Attached to the 6 x 12 Cylinders

Figure 3-19: Creep Cylinders Tower

Figure 3-20: Hydraulic Jack Placement for Loading

3.6.1 Creep and Shrinkage Data Collection

The vibrating wire strain gages are then used to collect all the creep and strain data from the 6 x 12 loaded cylinder and the 6 x 12 free shrinkage cylinders. The strain gages are embedded at 120 degrees from each other as shown in the figure 3-19 to record the strains all around the cylinder. All the strain readings are collected for analysis. There are three strain gages in each creep and free shrinkage 6 x 12 cylinder, so for five cylinders, there is a total of 15 strain gages, 9 for creep strains, and 6 for free shrinkage strains. All the vibrating strain gages wires were connected to a Campbell Scientific Loggernet System, which includes two AM16/32s multiplexers, one CR1000, and an

AVW200s as presented in figure 3-20 The system is placed in the environmental chamber by the creep rigs, and the data can be collected from the system using a normal USB cable. The strain data are exported on a laptop and formatted properly to be analyzed on Microsoft Excel. The average strain readings for the creep and free shrinkage samples are then calculated for analysis. Any readings collected from the strain gages that seems unreasonable due to sensor malfunction were disregarded.

Next, the vibrating wire strain gages are used to collect data from both the 6 x 12 creep and free shrinkage cylinders. To ensure that the strain is measured around the entire cylinder, the strain gages are placed at 120 degrees from each other as displayed in the figure 3-19. The stain measurements are collected and later used for analysis. For each of the two cylinders there are three strain gages; therefore, for five cylinders, there is a total of 15 gages. Out of the 15 strain gages, 9 are used for creep strains, and 6 for free shrinkage strains. The wires of the gages are attached to a Campbell Scientific Loggernet System, which should be stationed in the environmental chamber near the creep rigs. As shown in figure 3-21, the system includes two AM16/32s multiplexers, one CR1000, and an AVW200s. The system can also export data to a laptop using a USB cable. The data collected is then reformatted in Microsoft Excel and used to calculate the average strain measurements for both samples. Any inconsistent data that was due to sensor malfunction were not used.

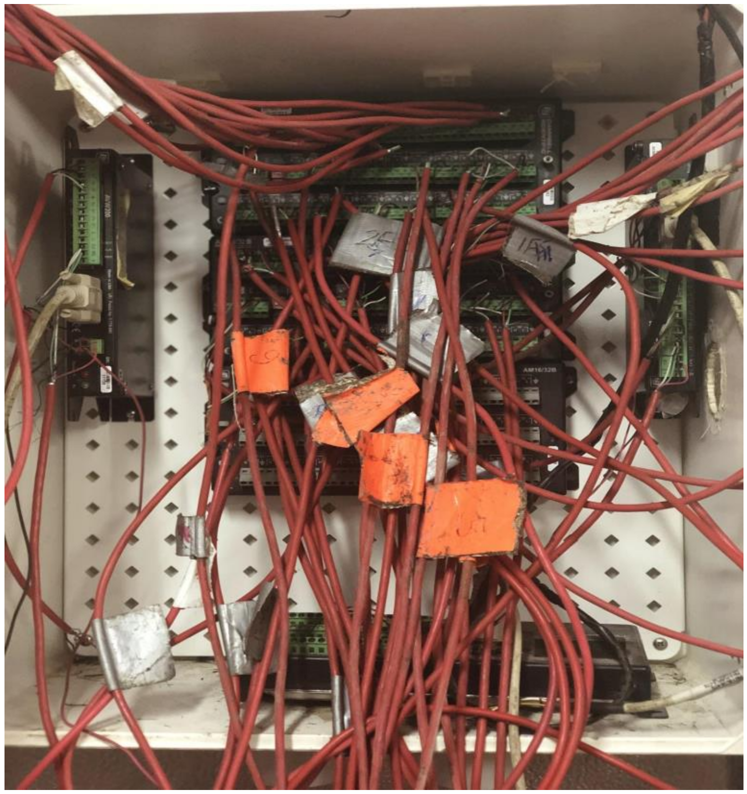

Figure 3-21: Campbell Scientific Loggernet System

CHAPTER IV
RESULTS AND ANALYSIS

4.1 Introduction

All the results collected for this research study will be presented in this chapter. Results of compressive strength, tensile strength, elastic modulus, free shrinkage, rapid chloride test, surface resistivity, and creep will be discussed, compared and analyzed for each mix.

4.2 Fresh Concrete Tests Results

Presented in table 4-1 the results for the slump and air content test for each mix.

Mixes	Slump (in)	Air Content (%)
HPC-FA-CR	6.5	7.1
HPC-FA-FR	4	6.4
HPC-HES-FA-CR	4	6
HPC-HES-FA-FR	4	7
HPC-HES-SL-CR	7.5	5
HPC-HES-SL-FR	7.5	5

Table 4-1: Fresh Concrete Test Results

4.3 Compressive Strength

Compressive strength test was performed on days 1, 7, 14, and 28 days for all mixes. Additional tests were done for HPC-HES mixes at 6 and 8 hours, to monitor concrete's high early strength. All the compression tests performed were done using 4 x 8 cylinder, but on 28 days, 6 x 12 cylinders were tested as well. Testing the 6 x 12 cylinders is necessary because creep cylinders were loaded up to 35% of their compression strength. All compressive strength results for all the mixes are shown in table 4-2 And figure 4-1.

Age (hrs, days)	HPC-FA-CR	HPC-FA-FR	HPC-HES-CR	HPC-HES-FA-FR	HPC-HES-SL-CR	HPC-HES-SL-FR
6 hrs			2695	1732	627	1823
8 hrs			3439	3177	2600	3101
1	2866	3113	4936	5016	5096	6290
7	4337	4268	7444	6931	6851	6847
14	4976	5096	6847	6799	8149	9236
28	6728	6568	7723	8360	8718	9713

Table 4-2: Compressive Test Results for 4 x 8 cylinder

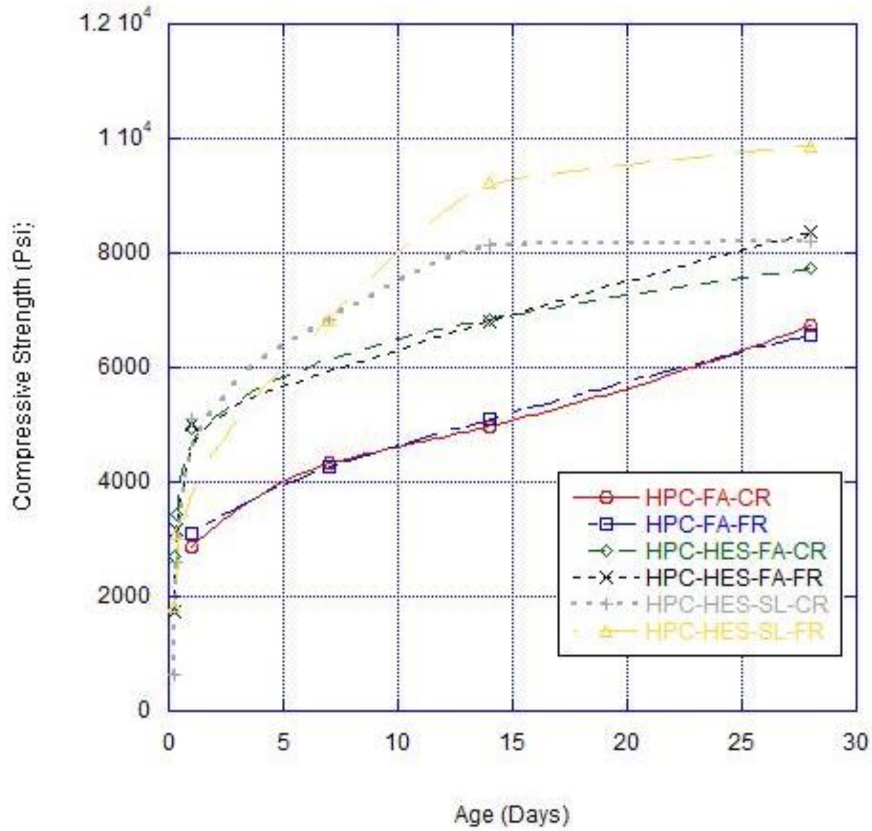

Figure 4-1: Compressive Test Results for 4 x 8 cylinders

Results shows a considerable increase in the compression strength of all HPC-HES mixes compared to HPC concrete. Moreover, HPC-HES gained higher compression strength at early age and also at 28 days. HPC-HES-FA-CR shows 14.8% increase in compressive strength increase with contrast with HPC-FA-CR at 28 days. HPC-HES-FA-FR shows 27.3% increase in compressive strength increase when compared with HPC-FA-FR. Similarly, HPC-HES-SL-CR had a 12.9% higher compressive strength with comparison to HPC-FA-CR. Furthermore, HPC-HES-SL-FR, had a 16.2% higher compressive strength with contrast to HPC-HES-FA-FR concrete mix. Fiber reinforcement does not show any noticeable effects to the compressive strength of the 4 x 8 cylinders.

Age (hr,days)	HPC-FA-CR	HPC-FA-FR	HPC-HES-FA-CR	HPC-HES-FA-FR	HPC-HES-SL-CR	HPC-HES-SL-FR
28	5006	5111	8099	7378	7742	7252

Table 4-3: Compressive Test Results for 6 x 12 cylinders

Correspondingly to the compressive testing of the 4 x 8 cylinders, the compressive strength of the 6 x 12 cylinders showed similar results as presented in table 4-3. HPC-HES-FA-CR and HPC-HES-FA-FR concrete mixes showed an increase in compressive strength with comparison to HPC-FA-CR and HPC-FA-FR of 61.8% and 44.3% respectively. Moreover, the HPC-HES-SL-CR and HPC-HES-SL-FR experienced an increase in compressive strength of 54.7% and 41.9% in contrast with HPC-FA-CR and HPC-FA-FR respectively.

4.3 Tensile Strength

Tensile strength tests were done on days 1, 7, 14, and 28 days for all mixes like compression tests. All tensile strength tests were performed on 4 x 8 cylinders till failure. Table 4-4 and Figure 4-2 present the tensile strength results obtained for all the concrete mixes tested.

Age (hr,days)	HPC-FA-CR	HPC-FA-FR	HPC-HES-CR	HPC-HES-FA-FR	HPC-HES-SL-CR	HPC-HES-SL-FR
1	342	392	342	438	547	578
7	427	427	552	510	552	585
14	454	512	558	587	617	644
28	618	649	607	653	717	742

Table 4-4: Tensile Test Results for 4 x 8 cylinder

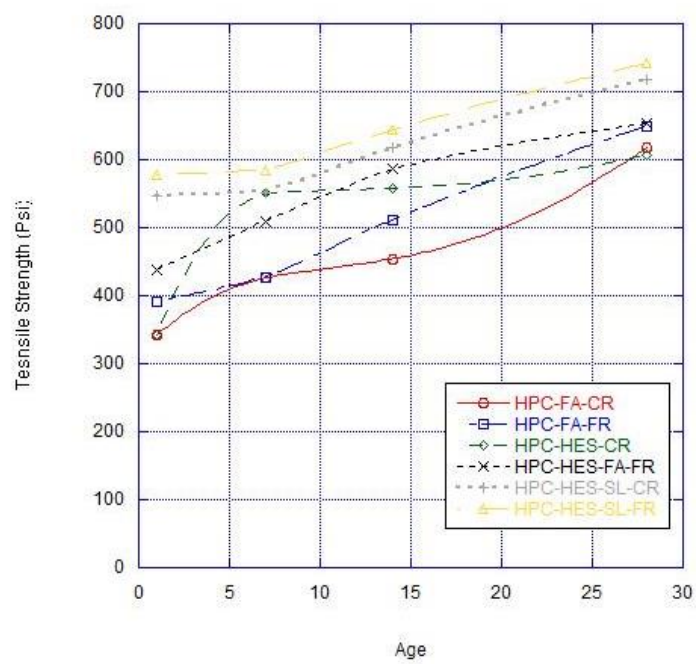

Figure 4-2: Tensile Test Results for 4 x 8 cylinder

All concrete mixes showed an increase in the tensile strength with the addition of polypropylene fibers as shown in table 4-4 and figure 4-2. HPC and HPC-HES concrete mixes gained a higher tensile strength that ranged from 5.0% to 7.6% increase with the addition of fiber reinforcements. In addition, it is observed that the use of slag cementitious improved the overall tensile performance of the HPC-HES concrete mixes, this increase was up to 18.1% in the control mix and 13.6% in the fiber reinforced mix.

Moreover, the fiber reinforced concrete mixes were able to sustain loads after failure. Concrete specimens with no fibers were brittle, split, and took zero loads after failure, as shown below. In conclusion, the addition of PE fibers noticeably increases the tensile strength of concrete, and also improve the ductility.

4.4 Elastic Modulus

Elastic modulus tests were performed on the same days as the tensile strength test. Results for the elastic modulus tests for all the mixes are shown in the table 4-5 and figure 4-3.

Age (hr,days)	**HPC-FA-CR**	**HPC-FA-FR**	**HPC-HES-CR**	**HPC-HES-FA-FR**	**HPC-HES-SL-CR**	**HPC-HES-SL-FR**
1	**3972**	**3853**	**3972**	**4802**	**4995**	**5591**
7	**4324**	**4335**	**3910**	**4739**	**5573**	**5631**
14	**4305**	**4525**	**4747**	**5283**	**5450**	**5862**
28	**4474**	**4584**	**5258**	**5064**	**5556**	**5742**

Table 4-5: Elastic Modulus Test Results

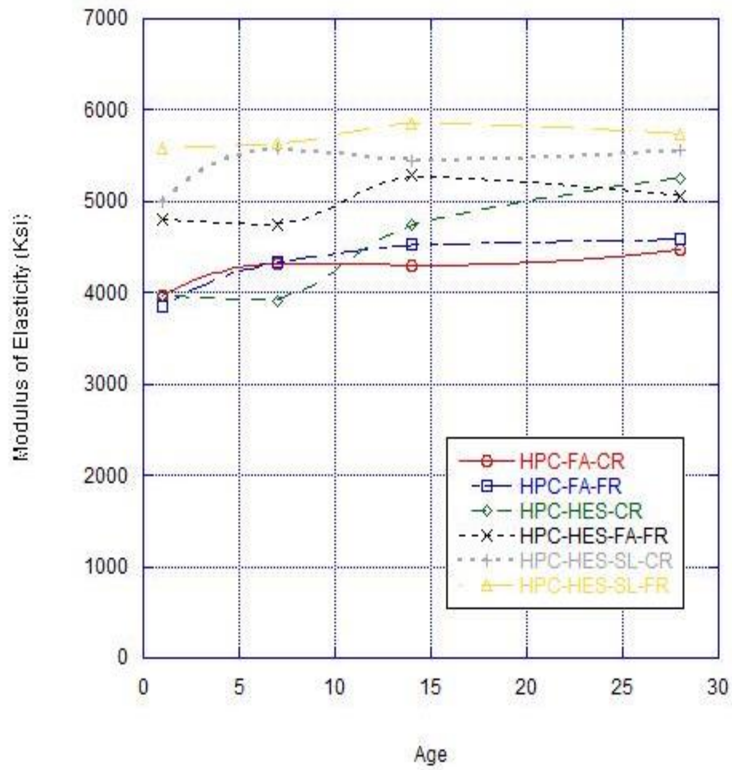

Figure 4-3: Elastic Modulus Test Results

The addition of fibers showed no considerable effects on the elastic modulus of concrete. HPC-HES mixes attained higher elastic modulus in overall compared to HPC mixes. Accelerating admixtures increase the elastic modulus by 17.5% and 10.5% for HPC-FA-CR and HPC-FA-FR respectively at 28 days. The use of SL in HPC-HES concretes increased the elastic modulus by 5.7% to 13.4% for HPC-HES concretes at 28 days.

4.6 Free Shrinkage

Free shrinkage tests were done for free shrinkage 3 x 3 prisms. The results obtained are presented in figure 4-3.

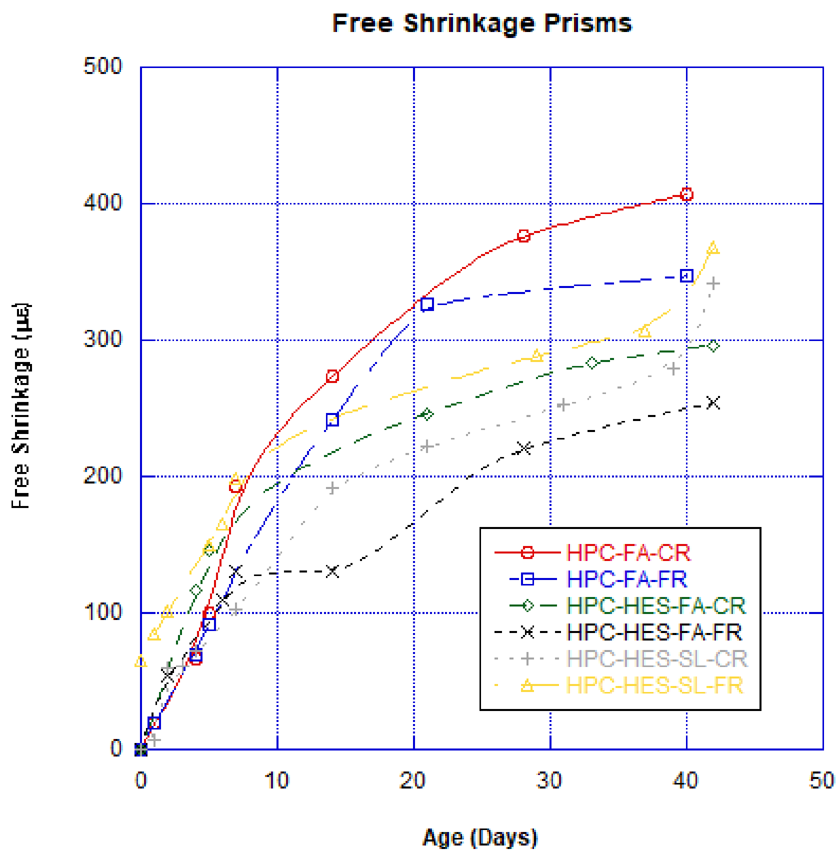

Figure 4-4: Free Shrinkage Test Results

Data collected revealed that fiber reinforcement using polypropylene fibers did not have significant effects on free shrinkage. The addition of polypropylene fiber reinforcement in all the mixes resulted in different effects in terms of shrinkage behavior. With that said, the overall changes of shrinkage did not exceed 8.6% in any of the mixes with the after the addition of fiber. HPC-HES-SL concretes showed a dramatic increase in the shrinkage of the concrete compared to HPC-HES-FA of 17.9% and 37.8% for the plain and fiber reinforced concrete respectively.

4.5 Surface Resistivity

Data for the surface resistivity test executed on days 7, 14, 28 and 56 are presented in the table 4-6.

Age (days)	HPC-FA-CR	HPC-FA-FR	HPC-HES-CR	HPC-HES-FA-FR	HPC-HES-SL-CR	HPC-HES-SL-FR
7	11.3	11.8	11.7	11.6		
14	15.6	15.8	17.7	20.5	29.6	32.3
28	24.2	26.3	36.5	33.4	39.3	48.2
56	44.5	43.2	59.75	60.85	45.5	55.9

Table 4-6: Surface Resistivity Test Results

Surface resistivity tests presented higher SR values for all HPC-HES concrete mixes, which means that they have better surface resistivity than normal HPC mixes. Improvement of surface resistivity was noticeable only after 7 days of curing. The SR test showed that fiber has insignificant effects on HPC and HPC-HES FA concrete mixes. On the other side, HPC-HES-SL-FR showed 22.9% better permeability with comparison to HPC-HES-SL-CR. In other words, polypropylene fiber reinforcement improves the permeability of HPC-HES-SL concrete mixes.

4.5 Rapid Chloride Test

RCPT test was only done after 28 and 56 days of casting. The result for the RCPT tests are shown in table 4-6.

Age (days)	HPC-FA-CR	HPC-FA-FR	HPC-HES-CR	HPC-HES-FA-FR	HPC-HES-SL-CR	HPC-HES-SL-FR
28	1654	1796	1256	1728	1283	1273
56	1428	1290	960	766	990	884

Table 4-6: Surface Resistivity Test Results

All the results obtained from the RCPT test at 28 days indicated low permeability based on ASTM C1202 range. At 56 days HPC-FA concrete mixes showed low permeability as well, on the other hand, all HPS-HES concrete mixes had very low permeability. Results prove that HPS-HES concrete has better resistance to chloride permeability than HPC mixes. The addition of fibers did not show any correlation with the permeability of the concrete mixes.

4.6 Shrinkage Strains and Specific Creep.

In this section the data collected from the free shrinkage and creep 6 x 12 cylinders will be discussed and analyzed.

4.6.1 Comparison of HPC Mixes

A full comparison between the two HPC concrete mixes with fiber reinforcement being the only variable between both mixes, was inspected in terms of free shrinkage and creep. HPC-CR being the control mix and HPC-FR being the fiber-reinforced. Figures 4-5 and 4-6 show the data collected for free shrinkage 6 x 12 cylinder using the VWSG for the HPC-CR and HPC-FR concretes.

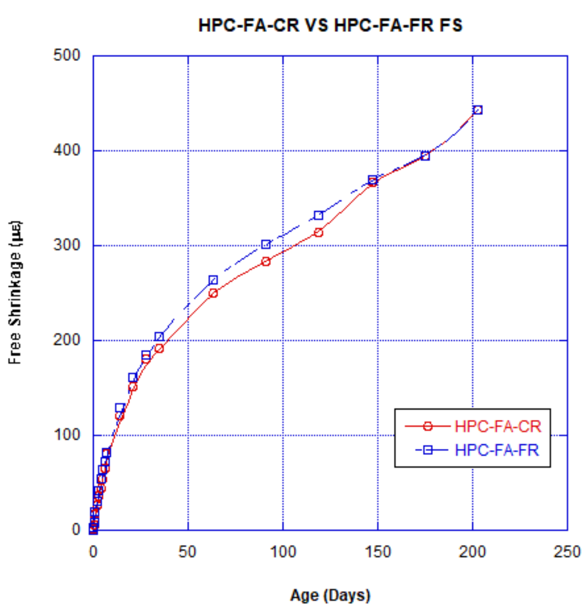

Figure 4-5: HPC Free Shrinkage

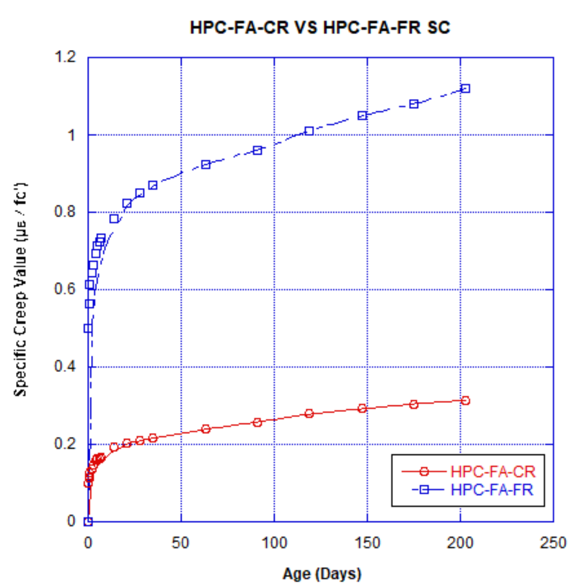

Figure 4-6: HPC Specific Creep

It was concluded that fiber reinforcement did not have significant effects on the 6 x 12 free shrinkage concrete cylinders similar to the data collected from the free shrinkage prisms.

Even though the fiber reinforcement did not affect the shrinkage of the 6 x 12 cylinders, but it increased the overall specific creep of the HPC-FA concrete by 257.8% at 203 days.

Collected data shows that fiber reinforcement has minimal effects on the shrinkage behavior of the concrete, but it significantly increases creep deformation. Results proof that there is a direct correlation between effects of the fiber reinforcement of the polypropylene fibers and the loading of the concrete specimens, which develop high creep strains.

4.6.2 Comparison of HPC-HES Fly Ash Mixes

Similarly, free shrinkage and creep results were investigated as shown in figures 4-7 and 6-7 for HPC-HES-FA-CR and HPC-HES-FA-FR concrete mixes.

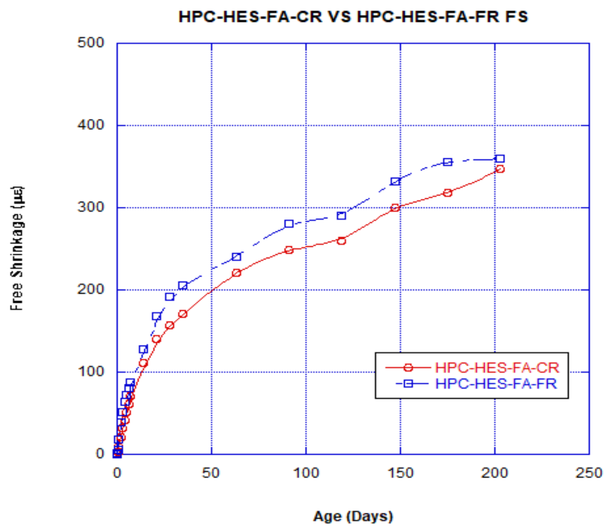

Figure 4-7: HPC-HES-FA Free Shrinkage

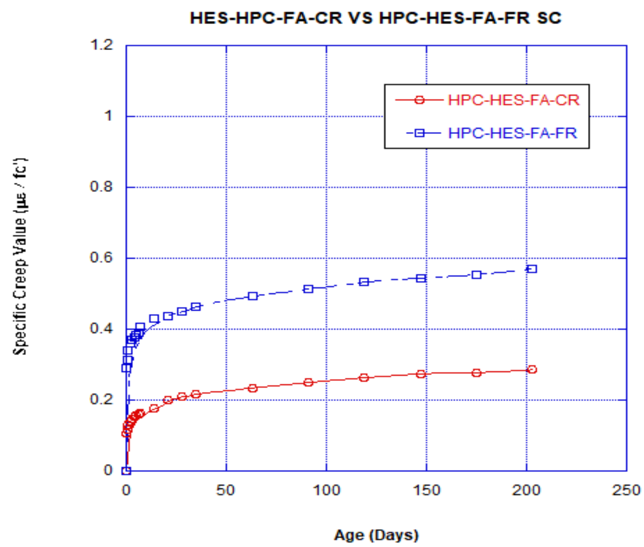

Figure 4-8: HPC-HES-FA Specific Creep

In a similar way to HPC concrete mix, fiber reinforcement had minimal effects on the free shrinkage of the HPC-HES concrete. HPC-HES-FA-FR concrete experienced only 3.5% increase in shrinkage in comparison to HPC-HES-FA-CR concrete mix.

On the other hand, polypropylene fiber reinforcement increased the specific creep deformation in HPC-HES concrete mixes. Results correspond to the data collected for the HPC concrete. In the case of HPC-HES concrete, fiber reinforcement increases specific creep by 99.3% at 203 days.

Shrinkage and creep results obtained from the HPC-HES concrete mixes proves that there is a direct relationship between the addition of fibers and a dramatic increase in creep strains due to applied stresses. Moreover, it is noticeable that the use of accelerators in high early strength concrete helped lower the increase of creep deformation with the addition of polypropylene fibers.

4.6.3 Comparison of HPC-HES Slag Mixes

A comparison of free shrinkage and specific creep data of the HPC-HES-SL-CR and HPC-HES-SL-FR was performed, as shown in figures 4-9 and 4-10.

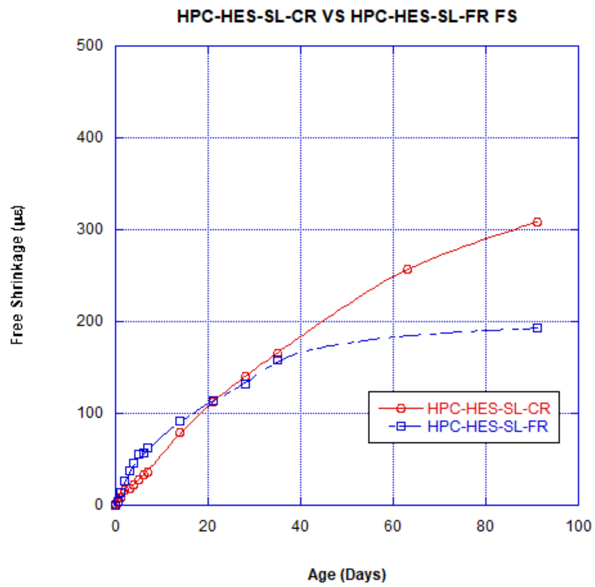

Figure 4-9: HPC-HES-SL Free Shrinkage

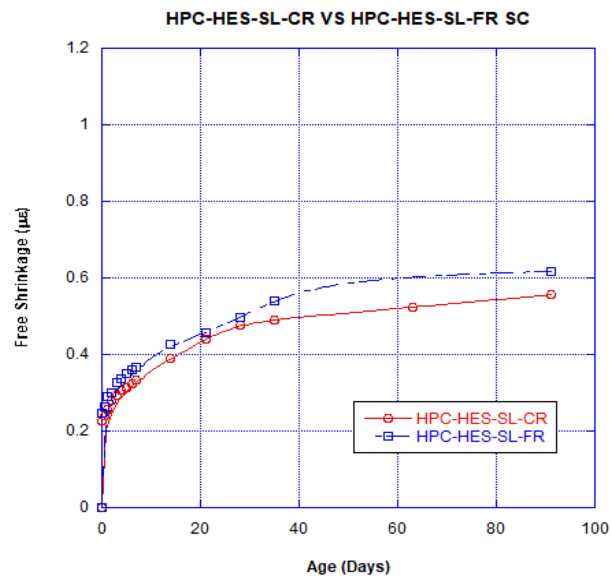

Figure 4-10: HPC-HES-SL Specific Creep

For the HPC-HES-SL mixes, the polypropylene fiber reinforcement dramatically decreased the free shrinkage of the concrete. HPC-`HES-SL-FR experienced 81% less shrinkage compared to the HPC-HES-SL-CR concrete.

Moreover, data indicates that polypropylene fiber reinforcement does not have significant effects on specific creep deformation of HES-HPC-SL concrete mixes. The addition of fibers in the HPC-HES-SL concrete only increased specific creep by 11.7% at 91 days, which is the least increase compared to the other fiber reinforced concrete mixes tested in this research study.

4.6.4 Comparison of HPC and HPC-HES Concrete Mixes

A contrast was made between HPC-FA and HPC-HES-FA concrete mixes for free shrinkage and specific creep deformations as shown in figures 4-11 and 4-12.

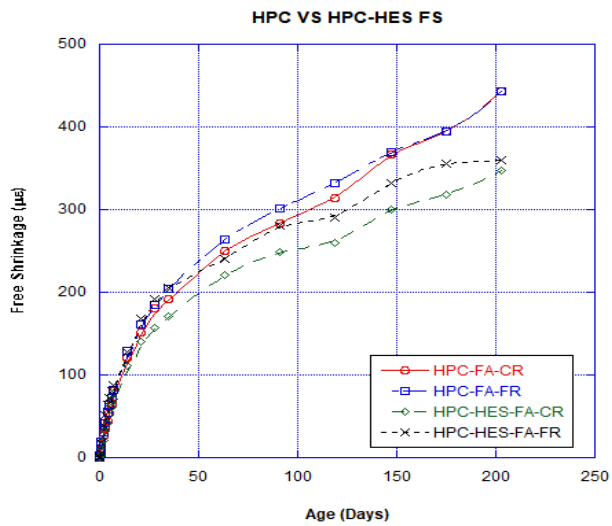

Figure 4-11: HPC-FA VS HPC-HES-FA FS

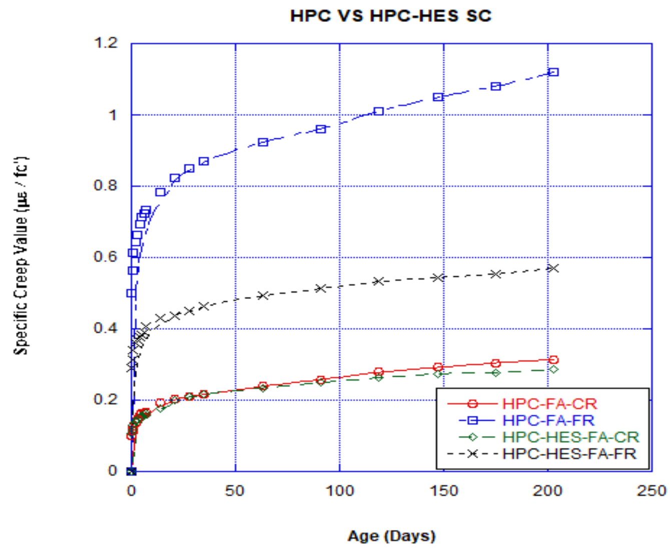

Figure 4-12: HPC-FA VS HPC-HES-FA SC

Data analyzed shows that HPC-HES-FA concretes experience less shrinkage than HPC-FA concrete mixes. HPC-FA-CR experienced 27.7% more shrinkage at 203 days than HPC-HES-FA-CR. Moreover, HPC-FA-FR experiences 23.4% higher shrinkage than HPC-HES-FA-FR at 203 days.

For specific creep deformation, HPC-FA-CR showed slightly higher deformation than HPC-HES-FA-CR, but the difference is insignificant. On the other hand, when HPC-FA-FR, and HPC-HES-FA-FR were compared, it was observed that the high early strength concrete mix underwent 49.1% less creep deformation.

With that said, the addition of accelerating admixture was the only difference between HPC and HPC-HES concrete mixes, therefore, the results proof that the addition of accelerators decreases free shrinkage, and creep deformation. The effects of the accelerating admixtures in decreasing creep strains was dramatically more effective than the decrease shown in shrinkage behavior.

4.6.5 Comparison of HPC-HES-FA and HPC-HES-SL Concrete Mixes

Moreover, a comparison was made between HPC-HES-SL and HPC-HES-FA concrete mixes at earlier ages as shown in figures 4-12 and 4-13.

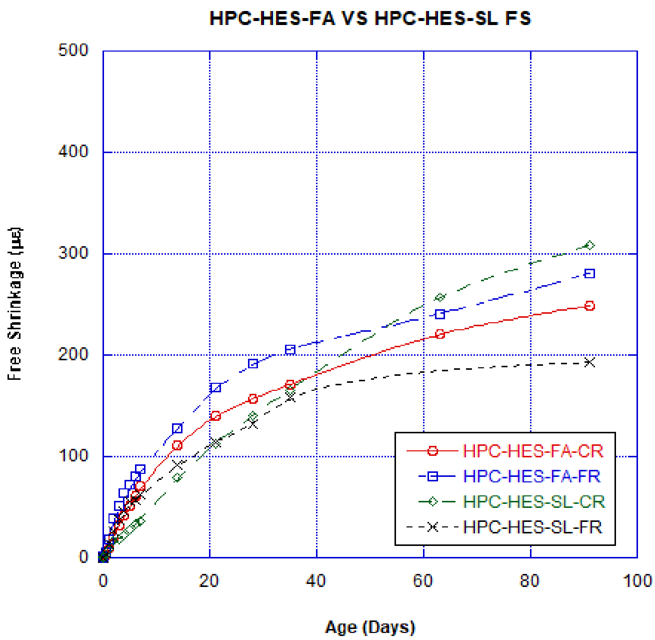

Figure 4-12: HPC-HES-FA VS HPC-HES-SL FS

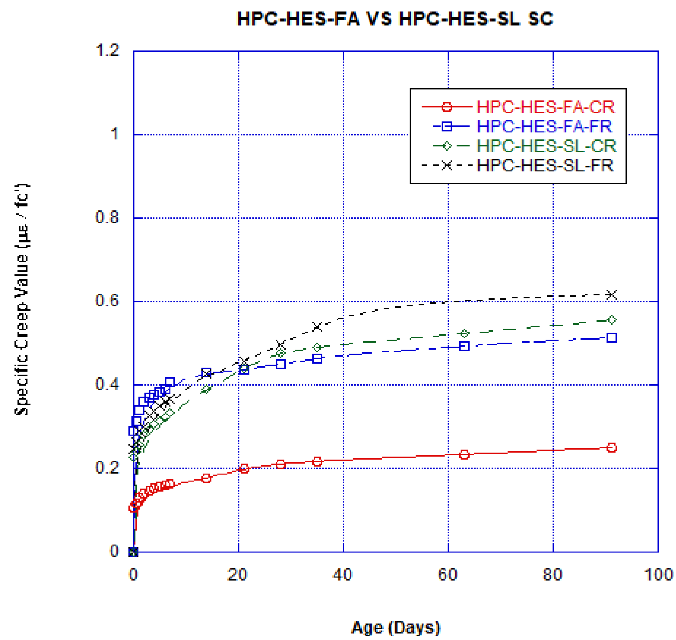

Figure 4-13: HPC-HES-FA VS HPC-HES-SL SC

For free shrinkage, HPC-HES-SL-CR specimen underwent 23.6% more free shrinkage than HPC-HES-FA-CR samples. Never the less, HPC-HES-FA-FR experienced 45.6% higher shrinkage at 91 days in comparison for HPC-HES-SL-FR concrete

Finally, HPC-HES-FA and HPC-HES-SL mixes were analyzed for creep deformation. It was observed that HPC-HES-FA-CR out preform HPC-HES-SL-CR concrete in terms of specific creep, since HPC-HES-SL-CR samples experienced 106.0% more creep deformation than HPC-HES-FA-CR specimens at 91 days. For the fiber reinforced mixes, HPC-HES-FA-FR concrete and HPC-HES-SL-FR concretes preformed similarly, as HPC-HES-SL-FR mix deformed 17.0% more than HPC-HES-FA-FR concrete in terms of specific creep at 91 days. Results presented shows that HPC-HES-FA mixes outperform HPC-HES-SL concrete in terms of creep for both plane and fiber reinforced mixes.

CHAPTER V

5.0 Models VS Experimental Specific Creep

ACI current creep prediction models were used to model the creep compliance for all the concrete mixes tested in this research study. ACI209R-92, B3, CEB MC90-99, and GL2000 models were all calculated and compared to the experimental results obtained for creep strains.

5.1 Models VS Experimental Creep: HPC, HPC-HES-FA and HPC-HES-SL Plane Mixes

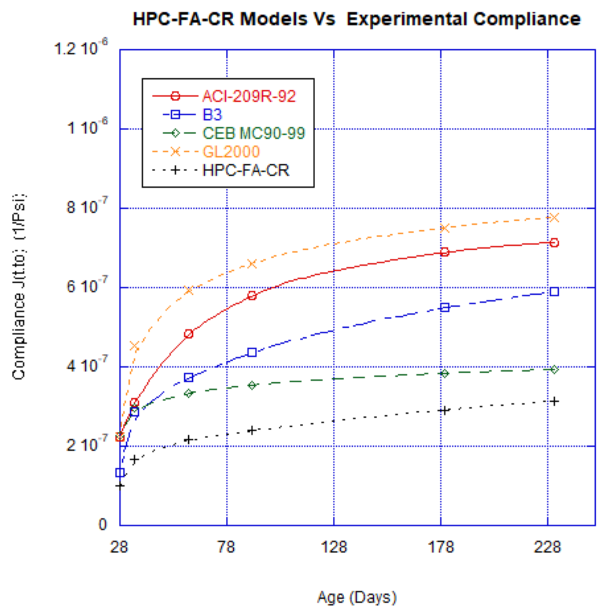

Figure 5-1: HPC-FA-CR Models VS Experimental

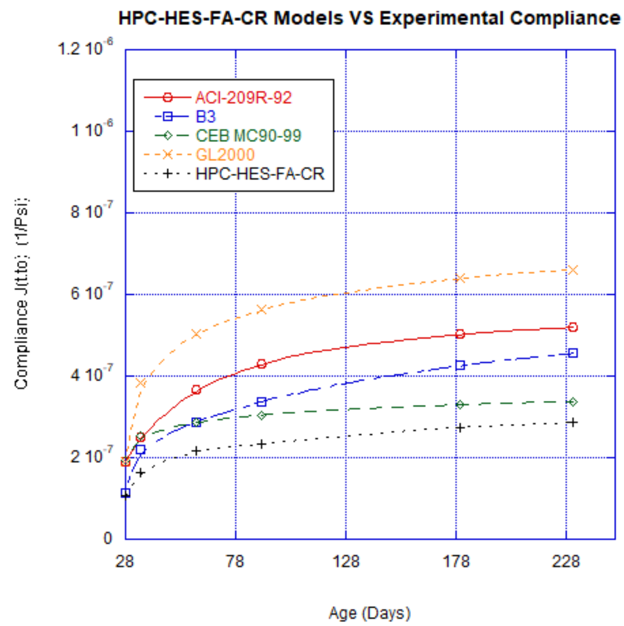

Figure 5-2: HPC-HES-FA-CR Models VS Experimental

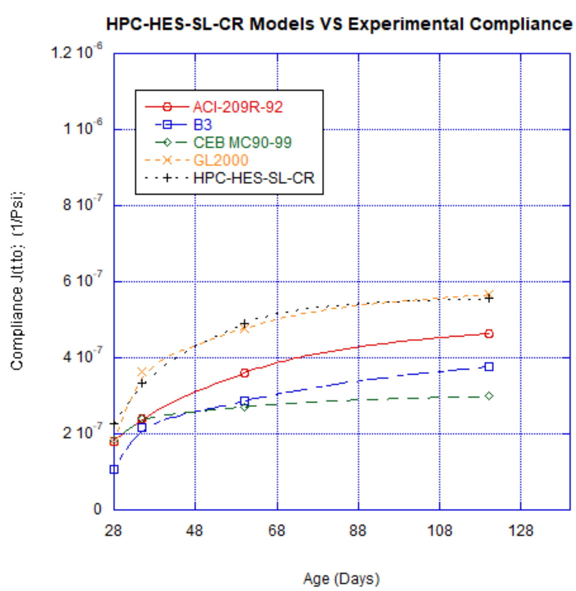

Figure 5-3: HPC-HES-SL-CR Models VS Experimental

Figures 5-1,5-2 and 5-3 presents the comparison between the creep prediction models and the experimental data collected in the lab. It is obvious that all the prediction models used to model creep compliance are conservative. ACI209R-92, B3, CEB MC90-99, and GL2000 models predict 128.0%, 88.0%, 24.5%, and 148.0% more creep than the experimental data for HPC-FA-CR mix at 231 days. Similarly, ACI209R-92, B3, CEB MC90-99, and GL2000 models predicted 81.5%, 59.1%, 18.2%, and 130.8% more creep in comparison to the actual experimental results of HPC-HES-FA-CR concrete at 231 days. On the other hand, HPC-HES-SL experienced creep strain which are with 10.25% of GL2000 creep model prediction. HPC-HES-SL underwent 11.5%, 36.4%, 72.1% more creep deformation after 91 days of loading than modeled by ACI-209R-92, B3, and CEB-MC90-99 respectively. Data shown concludes that CEB-MC90 creep prediction model is the closest to experimental results for HPC and HPC-HES fly ash control mixes, and GL2000 is the best model for HPC-HES slag plane mixes.

It is suggested to use CEB MC90-99 model to predict creep deformation for fly ash HPC and HPC-HES control mixes. It is suggested that the 24.5% error resulting from the CEB MC90-99 creep modeling of HPC-FA-CR mix is due to the use of FA as a partial substitute for cement, since the CEBMC90-99 does not consider the use of parital cementitious materials. Similarly, the 18.2% offset calculated by the CEB MC90-99 model for the HPC-HES-FA-CR is suggested to be due to inconsideration of the model to the use of FA and accelerating admixtures in the concrete mix.

5.2 Models VS Experimental Creep: HPC, HPC-HES-FA and HPC-HES-SL Fiber Reinforced Mixes:

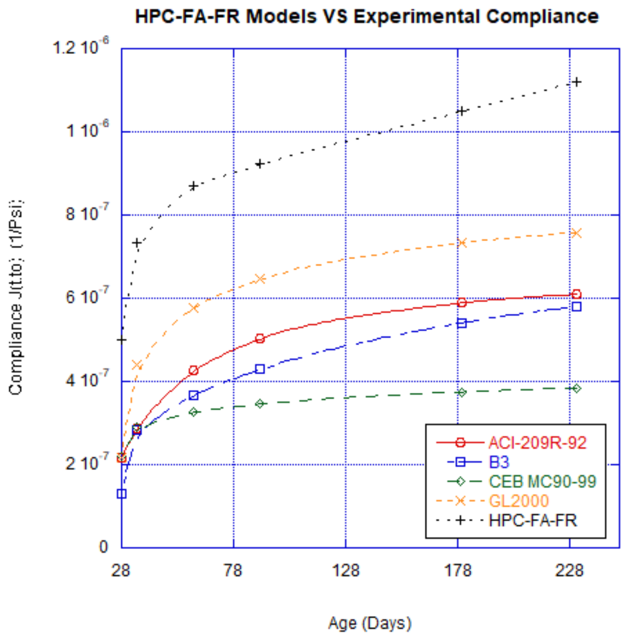

Figure 5-4: HPC-FA-FR Models VS Experimental

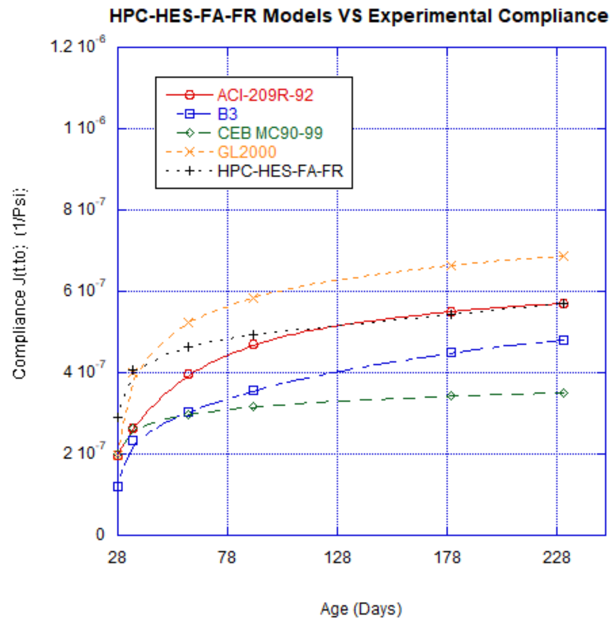

Figure 5-5: HPC-HES-FA-FR Models VS Experimental

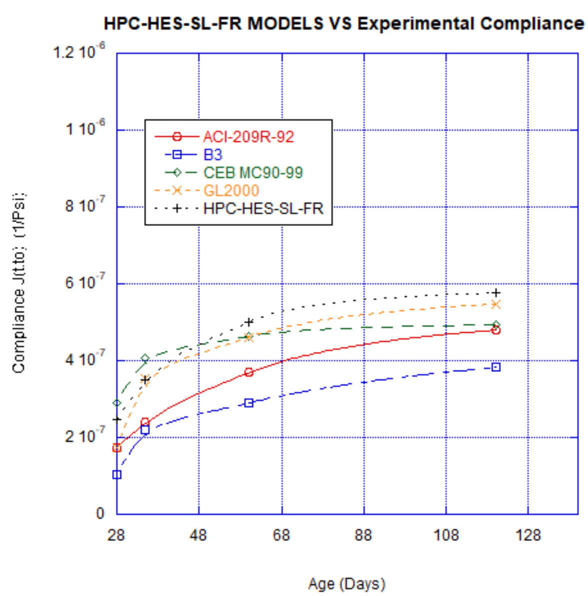

Figure 5-6: HPC-HES-SL-FR Models VS Experimental

Similarly, HPCF-FA-FR, HPC-HES-FA-FR, and HPC-HES-SL-FR concrete mixes were compared to the prediction models as presented in figures 5-4,5-5 and 5-6. Experimental results showed that HPC-FA-FR experienced 83.6%, 93.1%, 194.7%, and 47.8% more creep deformation at 231 days after loading with comparison to ACI209R-92, B3, CEB MC90-99, and GL2000 models. For the HPC-HES-FA-FR concrete mix, ACI 209R-92 model predicted the exact creep deformation as collected from the experimental data at 231 days. On the other hand, B3 and CEB-MC90-99 predicted a 15.9% and 38.7% less creep strains respectively with comparison to the experimental results for HPC-HES-FR-FR at 120 days. GL200 model predicted a 19.0% higher creep deformation in contrast to the experimental data after 231 days of loading. HPC-HES-SL-FR concrete experimental creep results show 20.2%, 50.6%, 100.3%, and 5.5% more creep than predicted by ACI209R-92, B3, CEB MC90-99, and GL2000 models respectively. Results show that for HPC-HES-FA-FR and HPC-HES-SL-FR creep modeling, ACI 209R-92 and GL2000 predicted relevant creep compliance results.

Even though, some prediction models seem to predict close creep compliance to the results collected for lab testing, those models are not reliable to be used to predict creep for all fiber reinforced concretes. None of the prediction models consider fibers, accelerator, or cementitious substitutes as factors effects creep of concrete, even though this research study proves they have significant effects on creep deformation.

5.1 Conclusion

1. Polypropylene fiber reinforcement resulted in increase of creep deformation in all concrete mixes tested in this research. Increase in the deformation varied from 3% to 250%. The wide range of creep deformations in different concrete mixes proved the sensitivity of the phenomena to other variables such as liquid admixtures and cementitious materials.
2. Fiber reinforcement in HPC-FA concrete resulted in a dramatic 257% more creep deformation, similarly, fiber reinforced HPC-HES-FA concrete experienced 99.3% more creep strain after 231 days of loading. Results suggests that polypropylene fibers have significant effects on the creep strains of HPC-FA and HPC-HES-FA concrete mixes.
3. The use of accelerating admixtures has no significant effects on concrete's creep deformation.
4. HPC-HES-FA-FR concrete mix experienced 49.1% less creep deformation than HPC-FA-FR after 231 days. The decrease in creep compliance for the HPC and HPC-HES fly ash mixes was due to the addition of accelerating admixture since this was the only variable between both mixes. It is suggested that the gain of early age strength in HPC-HES-FA-FR concrete with the addition of accelerating admixtures help build a stronger bond between the concrete and the fiber reinforcement. The bond improvement resulting from the addition of accelerators helps in lowering the high addition of creep strains resulting from the use of polypropylene fibers.

5. The use of SL instead of FA as a partial substitute for cement in HPC-HES concrete mixes resulted in an increase in creep deformation of 106.0% of in plane mixes and 17.0% in fiber reinforced mixes after 91 days of loading. FA showed an overall performance than the SL.
6. CEB MC90-99 gave the best prediction for HPC and HPC-HES control mixes. Moreover, ACI-20-92R and GL2000 prediction models results were within 5.5% range to the data experimentally collected for HPC-HES-FA-FR and HPC-HES-SL-FR respectively.
7. It is recommended to adjust the CEB MC90-99 model to add partial cementitious, accelerating admixture, and fibers material and content as factors in the model, to improve creep compliance predictions.

CHAPTER VI

6.0 Bibliography

Acker, Paul, and Ulm, Franz-Josef .“Creep and shrinkage of concrete: physical origins and practical measurements.”Procedia Engineering, Elsevier, 31 January 2001.

ACI209.2R. Guide for Modeling and Calculating Shrinkage and Creep in Hardened Concrete. May 2008.

Aitcin, Pierre-Claude, and Barbara B. Stern. High-Performance Concrete. E & FN Spon, 1998.

Al-Manaseer , A A. “Creep of Concrete Containing Fly Ash and Superplasticize at Different Stress/Strength Ratios.” ACI Journal Proceedings, vol. 83, no. 4, 1986, doi:10.14359/10660.

Al-Manaseer, Akthem, and Jian-Ping Lam. “Statistical Evaluation of Shrinkage and Creep Models.” ACI Materials Journal, vol. 102, no. 3, 2005, doi:10.14359/14444.

Barborak, Ryan. Fiber Reinforced Concrete (FRC) DMS-4550 Tip Sheet . Jan. 2011.

Bažant, Z. P. “Creep Stability and Buckling Strength of Concrete Columns.” Magazine of Concrete Research, vol. 20, no. 63, June 1968, pp. 85–94., doi:10.1680/macr.1968.20.63.85.

Bažant, Zdenêk P., and Xi Yunping. “Drying Creep of Concrete: Constitutive Model and New Experiments Separating Its Mechanisms.” Materials and Structures, vol. 27, no. 1, 1994, pp. 3–14.

Baˇzant, Z.P. (2001). "Creep of Concrete." Complete version of an article whose slightly abbreviated version was printed in Encyclopedia of Materials: Science and Technology, K.H.J. Buschow et al., eds. Elsevier, Amsterdam, Vol. 2C, 1797–1800.

Branson, D. E., and Christiason, M. L., "Time Dependent Concrete Properties Related to Design—Strength and Elastic Properties, Creep and Shrinkage," Creep, Shrinkage and Temperature Effects, SP-27, American Concrete Institute, Detroit, MI, 1971, pp.257-277.

Brewer, Gregory. "Restrained Shrinkage Behavior of High Performance Concrete Reinforced with Synthetic and Steel Fibers." May 2018.

Brooks, J. J., and A. Neville. "Creep and Shrinkage of Concrete as Affected by Admixtures and Cement Replacement Materials." Special Publication, 1 Dec. 1992,

Brown, Noel H., and Brian B. Hope. "The Creep of Hydrated Cement Paste." Cement and Concrete Research, vol. 6, no. 4, July 1976, pp. 475–485.

Carrasquillo, Ramon L, et al. Properties of High Strength Concrete Subject to Short-Term Loads . 1981.

Castine, Stephanie, "Development of High Early-Strength Concrete for Accelerated Bridge Construction Closure Pour Connections" (2017). Masters Theses. 498.

Chowdhary, Peeyush, and Ravi K. Sharma. "Effect of Relative Humidity on Creep-Shrinkage Behaviour of Composite Tall Buildings." Latin American Journal of

Solids and Structures, vol. 10, no. 3, May 2013, pp. 571–584., doi:10.1590/s1679-78252013000300007.

Davis, R.E., and G. E. Troxell. 1954. Properties of concrete and their influence on prestress design.ACI JOURNAL, 50(23), 381-391

Dilger, W H, and C Wang. “Creep and Shrinkage of High-Performance Concrete .”

Du, Lianxiang, and Kevin J. Folliard. “Mechanisms of Air Entrainment in Concrete.” Cement and Concrete Research, vol. 35, no. 8, Aug. 2005, pp. 1463–1471.

EL Khoury, Raymond. “Creep and Shrinkage of Self-Consolidating Concrete.” Welcome to RUcore - Rutgers University Community Repository, 2010, rucore.libraries.rutgers.edu/rutgers-lib/30043/.

Farrington, Erik W., et al. CREEP AND SHRINKAGE OF HIGH PERFORMANCE CONCRETE. 1996, pp.1- 90.

Gambali, Ajay, and Naveen Shanagam. “Creep of Concrete.” International Journal of Engineering Development and Research, vol. 2, 2014.

Khadiranaikar , R B, and Bagalkot . “High Performance Concrete .”

GCP Applied Technologies Inc. Ground Granulated Blast-Furnace Slag: Its Chemistry and Use with Chemical Admixtures. Ground Granulated Blast-Furnace Slag: Its Chemistry and Use with Chemical Admixtures, GCP Applied Technologies, 2016.

Ghosh, Ram S, and John Timusk. “Creep of Fly Ash Concrete.” ACI Journal Proceedings, vol. 78, no. 5, 1981, doi:10.14359/10519.

Goel, Rajeev, et al. “Comparative Study of Various Creep and Shrinkage Prediction Models for Concrete.” Journal of Materials in Civil Engineering, vol. 19, no. 3, 2007, pp. 249–260.

Hansen, Torben C, and Alan H Mattock. “Influence of Size and Shape of Member on the Shrinkage and Creep of Concrete.”

Hauggaard, Anders Boe, et al. “Transitional Thermal Creep of Early Age Concrete.” Journal of Engineering Mechanics, vol. 125, no. 4, Apr. 1999, pp. 458–465.

He, Wenjun, "Creep and Shrinkage of High Performance Concrete, and Prediction of Long-Term Camber of Prestressed Bridge Girders" (2013). Graduate Theses and Dissertations. 13418. https://lib.dr.iastate.edu/etd/13418

Houde, J., et al. “Creep of Concrete Containing Fibers and Silica Fume.” Special Publication, 1 Dec. 1987,

Hover, Kenneth C. “Concrete Mixture Proportioning with Water-Reducing Admixtures to Enhance Durability: A Quantitative Model.” Cement and Concrete Composites, Elsevier, 5 Mar. 1999,

Jarosaw, Byszko.“Comparative analysis of creep in standard and fibre reinforced concretes under different load conditions.”Procedia Engineering, Elsevier, 29 June 2017, Joshi, Ramesh C., and Rajinder P. Lohtia. Fly Ash in Concrete: Production, Properties and Uses. Vol. 2, Gordon and Breach Science Publ., 1997.

Lluka, Diana, et al. “International Journal of Engineering Research and Technology (IJERT).” Effect of Relative Humidity on Creep and Shrinkage of Concrete According to the European Code for Calculation of Slender Columns, vol. 4, no. 10, ser. 2278-0181, Oct. 2015, pp. 466–472. 2278-0181

Nassif, Hani, et al. “Shrinkage Behavior of High Performance Concrete Cured Using Heat-Blanket.” Sciences Engineering Medicine, 2014.

Nemati, Kamran. “Volume Changes and Creep af Concrete.” 2006.

Neville, Adam M., and Bernard L. Meyers. “Creep of Concrete: Influencing Factors and Prediction.” Special Publication, 1 Jan. 1964.

Niyogi, A.k., et al. “The Influence of Age at Time of Loading on Basic and Drying Creep.” Cement and Concrete Research, vol. 3, no. 5, Sept. 1973, pp. 633–644., doi:10.1016/0008-8846(73)90100-2.

Polivka, M. P. (1964). Studies of creep in mass concrete. Paper 12, Symp. on Mass Concrete, ACI Special Publication, No.6, 30.

Qingxin Zhao, Junchao Yu, Guoqing Geng, Jinyang Jiang, and Xiaochen Liu. “Effects of fiber types on creep behavior of concrete.” Procedia Engineering, Elsevier, 28 Dec. 2015.

Rosskopf, PA, et al. “Effect of Various Accelerating Chemical Admixtures on Setting and Strength Development of Concrete.” Journal of Testing and Evaluation, ASTM International, 1 July 1975.

Sagara, Altho, and Ivindra Pane. “A Study on Effects of Creep and Shrinkage in High Strength Concrete Bridges.” Procedia Engineering, Elsevier, 23 Nov. 2015,

Schneider, Ulrich. “Concrete at High Temperatures — A General Review.” Fire Safety Journal, vol. 13, no. 1, 7 Apr. 1988, pp. 55–68.

Sennour, Mohand. “Creep and Shrinkage Properties in Concrete Containing Fly Ash.” Nov. 1989.

SHAH, SURENDRA, and B. VIJAYA RANGAN. Fiber Reinforced Concrete Properties. 1971.

Shahab, Samad, et al. “Strength Development Characteristics of Concrete Produced with Blended Cement Using Ground Granulated Blast Furnace Slag (GGBS) under Various Curing Conditions.” Indian Academy of Sciences, vol. 2, 7 July 2017, pp. 1203–1213.

Sohaib, N, et al. “Using Polypropylene Fibers in Concrete to Achieve Maximum Strength.” Eighth International Conference On Advances in Civil and Structural Engineering - CSE 2018, 2018, doi:10.15224/978-1-63248-145-0-36.

Tamtsia, Basile T, and James J Beaudoin. “Basic Creep of Hardened Cement Paste A Re-Examination of the Role of Water.” Cement and Concrete Research, vol. 30, no. 9, Sept. 2000, pp. 1465–1475.

Tazawa, E, et al. “Drying Shrinkage and Creep of Concrete Containing Granulated Blast Furnace Slag .” p. 1989.

Theiner, Y., et al. “Comprehensive Study of Concrete Creep, Shrinkage, and Water Content Evolution under Sealed and Drying Conditions.” Strain, John Wiley & Sons, Ltd (10.1111), 1 Feb. 2017, onlinelibrary.wiley.com/doi/pdf/10.1111/str.12223.

Whiting, D, and J Schmitt. Durability Of In-Place Concrete Containing High-Range Water-Reducing Admixtures . Sept. 1987.

Zhang, Liang Liang, et al. “Effect of Fly Ash on Creep of High Performance Concrete Used in Bridge.” Applied Mechanics and Materials, vol. 204-208, 26 Oct. 2012, pp. 2192–2195.

Zollo, Ronald F. “Fiber-Reinforced Concrete: an Overview after 30 Years of Development.” Cement and Concrete Composites, Elsevier, 20 May 1998